frontiers in Earth Science

ORIGINAL RESEARCH
published: 28 March 2022
doi: 10.3389/feart.2022.803505

New Ankylosaurian Cranial Remains From the Lower Cretaceous (Upper Albian) Toolebuc Formation of Queensland, Australia

Timothy G. Frauenfelder[1], Phil R. Bell[1], Tom Brougham[1], Joseph J. Bevitt[2], Russell D. C. Bicknell[1], Benjamin P. Kear[3], Stephen Wroe[1] and Nicolás E. Campione[1]*

[1]Palaeoscience Research Centre, School of Environmental and Rural Science, University of New England, Armidale, NSW, Australia, [2]Australian Centre for Neutron Scattering, Australian Nuclear Science and Technology Organisation, Sydney, NSW, Australia, [3]Museum of Evolution, Uppsala University, Uppsala, Sweden

OPEN ACCESS

Edited by:
Alejandro Serrano Martínez, Institut Català de Paleontologia Miquel Crusafont, Spain

Reviewed by:
Wenjie Zheng, Zhejiang Museum of Natural History, China
Ryan T. Tucker, Stellenbosch University, South Africa

***Correspondence:**
Timothy G. Frauenfelder
timothy.frauenfelder@gmail.com

Specialty section:
This article was submitted to Paleontology, a section of the journal Frontiers in Earth Science

Received: *28 October 2021*
Accepted: *10 January 2022*
Published: *28 March 2022*

Citation:
Frauenfelder TG, Bell PR, Brougham T, Bevitt JJ, Bicknell RDC, Kear BP, Wroe S and Campione NE (2022) New Ankylosaurian Cranial Remains From the Lower Cretaceous (Upper Albian) Toolebuc Formation of Queensland, Australia. Front. Earth Sci. 10:803505. doi: 10.3389/feart.2022.803505

Australian dinosaur research has undergone a renaissance in the last 10 years, with growing knowledge of mid-Cretaceous assemblages revealing an endemic high-paleolatitude Gondwanan fauna. One of its most conspicuous members is ankylosaurs, which are rare but nonetheless occur in most Australian dinosaur-bearing formations spanning the uppermost Barremian to lower Cenomanian. Here we describe a partial ankylosaur skull from the marine Toolebuc Formation exposed near Boulia in western Queensland, Australia. This skull represents the oldest ankylosaurian material from Queensland, predating the holotype of *Kunbarrasaurus ieversi*, which was found in the overlying Allaru Mudstone. The ankylosaur skull is encased in a limestone concretion with the maxillary tooth rows preserved only as impressions. Synchrotron radiation X-ray tomography was used to non-destructively image and reconstruct the specimen in 3D and facilitate virtual preparation of the separate cranial bones. The reconstruction of the skull revealed the vomer, palatines, sections of the ectopterygoids and maxillae, and multiple teeth. The palate has posteriorly positioned choanae that differs from the more anterior placement seen in most other ankylosaurians, but which is shared with *K. ieversi*, *Akainacephalus johnsoni*, *Cedarpelta bilbeyhallorum, Gobisaurus domoculus,* and *Panoplosaurus mirus*. Phylogenetic analyses place the new cranial material within the recently named basal ankylosaurian clade Parankylosauria together with *K. ieversi.* This result, together with the anatomical similarities to the holotype of *K. ieversi*, permits its referral to cf. *Kunbarrasaurus* sp. This specimen elucidates the palatal anatomy of Australian ankylosaurs and highlights one of the most ubiquitous components of Australian mid-Cretaceous dinosaur faunas.

Keywords: Ankylosauria, *Kunbarrasaurus*, Australia, *Minmi*, Cretaceous, Gondwana, Toolebuc Formation, synchrotron

INTRODUCTION

Ankylosaurians are a rare component of Gondwanan Cretaceous terrestrial ecosystems with five described species: *Antarctopelta oliveroi*, *Minmi paravertebra*, *Kunbarrasaurus ieversi*, *Spicomellus afer*, and *Stegouros elengassen* (Molnar, 1980; Salgado and Gasparini, 2006; Leahey et al., 2015; Maidment et al., 2021; Soto-Acuña et al., 2021). *A. oliveroi* and *M. paravertebra* have been considered *nomen dubia* due to a perceived lack of autapomorphies (Leahey et al., 2015; Arbour and Currie, 2016). However, comparisons between *M. paravertebra* and *K. ieversi* support their differentiation and the specific validity (Leahey et al., 2015). Despite the currently limited taxonomic diversity of Gondwanan Cretaceous ankylosaurs, skeletal fragments ascribed to the clade are found throughout Argentina (Coria and Salgado, 2001; Murray et al., 2019), New Zealand (Molnar and Wiffen, 1994), and Madagascar (Russel et al., 1976), with further ichnological evidence from Bolivia (Apesteguía and Gallina, 2011; Riguetti et al., 2021), and Brazil (Francischini et al., 2018). These widespread occurrences demonstrate that ankylosaurs were a rare yet pervasive component of Gondwanan dinosaur faunas. In Australia, ankylosaurian occurrences include two named taxa, *M. paravertebra* (Molnar, 1980) and *K. ieversi* (Molnar, 1996; Leahey et al., 2015), along with footprints (Salisbury et al., 2016) and several isolated skeletal elements that span most Australian dinosaur-bearing formations (Molnar, 1996; Molnar, 2001; Barrett et al., 2010; Leahey and Salisbury, 2013; Leahey et al., 2015; Bell et al., 2018a).

Despite brief mentions in the literature for almost 40 years, ankylosaurs from the middle–upper Albian marine Toolebuc Formation of central Queensland have never previously been studied in detail (Molnar, 1996; Leahey and Salisbury, 2013; Leahey et al., 2015). Three specimens were previously reported from two localities, Julia Creek (QM F33286) and Hughenden (AM F35259, AM F119849), and all were tentatively referred to the genus *Minmi* (**Figures 1A,B**; Molnar, 1996). QM F33286 is a partially disarticulated ankylosaur comprising "thoracic and pelvic" elements associated with ventral or lateroventral dermal ossifications (Molnar, 2001; Leahey and Salisbury, 2013). A brief report mentioned that the dermal ossicles were tightly arranged as square tiles that presumably covered most of the neck and trunk (Molnar, 2001). AM F35259 includes only a series of incomplete ribs with ossicles. AM F119849 likewise comprises a single block with vertebrae, ribs, and dermal ossifications (Leahey and Salisbury, 2013).

Here we provide the first comprehensive description of ankylosaur cranial remains recovered from the Toolebuc Formation based on a previously undocumented specimen, SAMA P40536, collected by BPK in 2005 from Warra Station near Boulia in western Queensland. SAMA P40536 is preserved within a series of yellow limestone concretions typical of the Toolebuc Formation (Kellner et al., 2010) but had eroded out and were dispersed throughout the blacksoil weathering residuum. The concretions contain remnants of the skull, pelvis, and limbs associated with isolated vertebrae, ribs, and dermal armor fragments. Our initial assessment of the remains focuses on the cranium and dentition, which are important because they represent only the second example of an ankylosaur skull recovered from Australia to date.

INSTITUTIONAL ABBREVIATIONS

QM, Queensland Museum, Brisbane, Queensland, Australia; SAMA, South Australian Museum, Adelaide, South Australia, Australia; AM, Australian Museum, Sydney, New South Wales, Australia.

METHODS FOR SYNCHROTRON SCANNING AND 3D MODELING

Microtomographic measurements of SAMA P40536 were performed using the Imaging and Medical Beamline (IMBL) at the Australian Nuclear Science and Technology Organisation's (ANSTO) Australian Synchrotron, Melbourne, Victoria, Australia. For this investigation, acquisition parameters included a 40.29 × 40.29 μm pixel size, monochromatic beam energy of 70 keV, a sample–detector distance of 500 mm, and the "Ruby" detector. The latter consists of a PCO. edge sCMOS camera (16-bit, 2,560 × 2,160 pixels) and a Nikon Makro Planar 100 mm lens coupled with a 20 μm thick Gadox/CsI(Tl)/$CdWO_4$ scintillator screen. As the height and width of the specimen exceeded the detector field-of-view, the specimen was aligned axially relative to the beam, its center of rotation shifted toward one edge of the detector. Twelve successive scans were required to cover the full specimen volume, each consisting of 1,500 equally spaced angle shadow radiographs with an exposure length of 0.35 s, obtained every 0.12° as the sample was continuously rotated 180° about its vertical axis. Horizontal translation of the specimen between tomographic scans was 80 mm, and 25 mm between vertical scans. One-hundred dark (closed shutter) and beam profile (open shutter) images were obtained for calibration before and after shadow-radiograph acquisition. The total time for the scan was 140 min.

The raw 16-bit radiographic series were normalized relative to the beam calibration files and stitched with the in-house software "IMBL-Stitch" to yield a 32-bit series with a 178 × 160 mm field-of-view. Reconstruction of the 3D dataset was achieved by the filtered-back projection method using the CSIRO's X-TRACT (Gureyev et al., 2011). The image stack (Available on MorphoSource; ark:/87602/m4/392687) was segmented, and the volume data was rendered using Mimics Innovation Suite (v. 21.4; Materialise HQ, Leuven, Belgium). As various sections are preserved as bone impressions, with the original bone lost, thin surface models (~0.8 mm thick) were added during segmentation to illustrate the relative placement of these bones. Finally, to create positive molds of the tooth row and properly study the dental anatomy, the negative left dentary tooth row impression was molded in Pinkysil® (fast set silicone) and cast in Easycast® (Rigid Polyurethane System). Manual preparation techniques using an air scribe (Paleotools® Micro Jack 3) were used to extract a single preserved tooth crown,

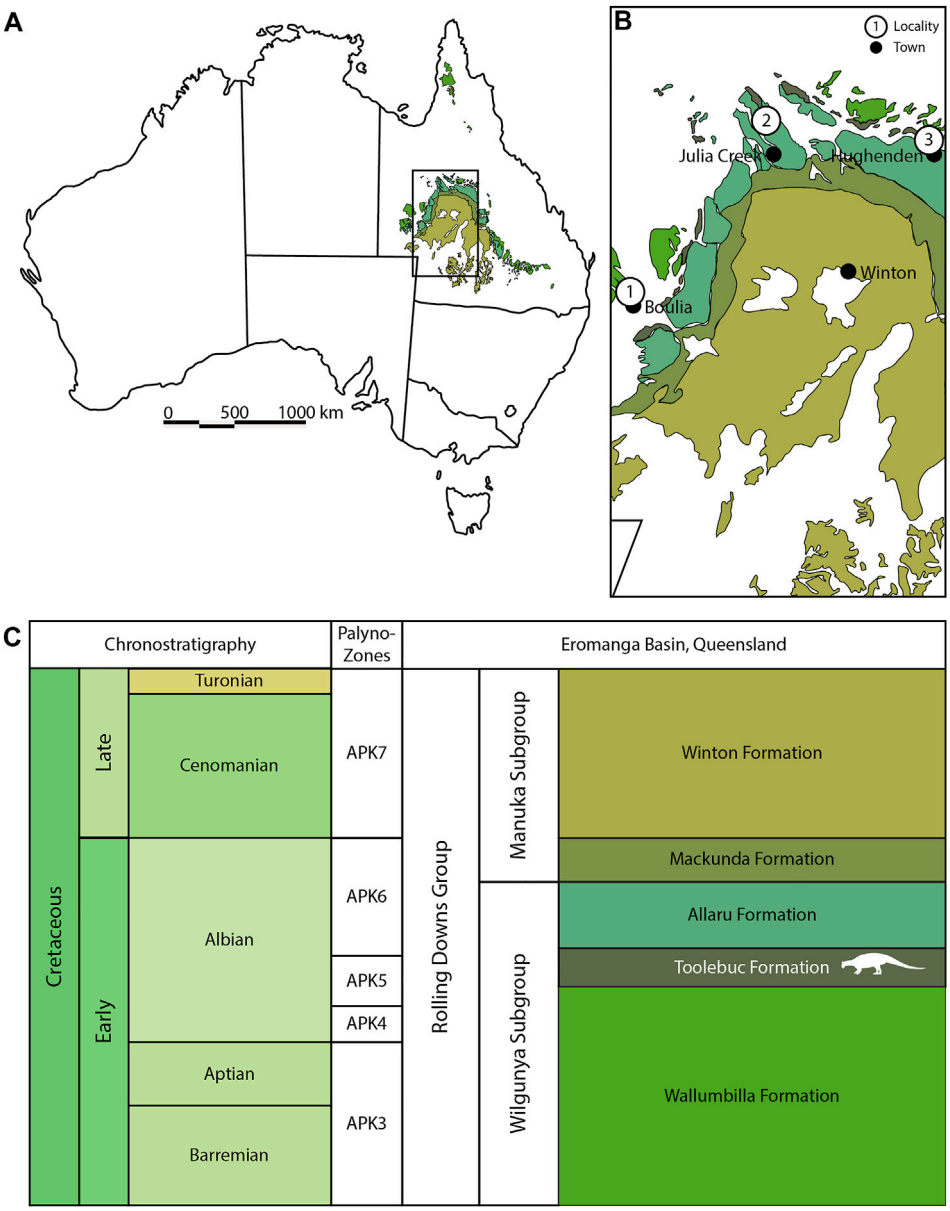

FIGURE 1 | Spatiotemporal context of the Eromanga Basin, Queensland, Australia. **(A)** Map of Australia with Eromanga Basin formations highlighted, based on Pentland and Poropat (2019). **(B)** Toolebuc Formation ankylosaur localities.1—SAMA P40536 location, near Boulia (this study); 2—QM F33286 location, near Julia Creek; 3—AM F35259 and AM F119849 location, near Hughenden. Ankylosaur locations based on Leahey et al. (2015). **(C)** Chronostratigraphy of the Eromanga Basin, highlighting the mid-Albian Toolebuc Formation (in white). Formation colors match **(A)** and **(B)**, based on Cavin and Berrell (2019). Ankylosaur silhouette generated by Jagged Fang Designs and reused under Creative Commons licenses: Public Domain Dedication 1.0.

subsequently scanned using the General Electric (GE) Phoenix V|tome|xs microCT scanner at the University of New England, Armidale. This tooth did not show in the original synchrotron scan.

SYSTEMATIC PALAEONTOLOGY

Dinosauria Owen, 1842
Ornithischia Seeley, 1888
Thyreophora Nopcsa, 1915
Ankylosauria Osborn, 1923
Kunbarrasaurus Leahey et al., 2015
cf. *Kunbarrasaurus* sp.

Referred Material—SAMA P40536, a partial skull incorporating impressions of the left and right maxillae, the vomer, both palatines, the right (and part impression of the left) ectopterygoid, a possible right mandibular ramus, impressions of both maxillary tooth rows, and eight isolated teeth (**Supplementary**

Materials S1, S2 available at figshare; https://figshare.com/articles/figure/3D_PDF_of_SAMA_P40536-_Frauenfelder_et_al_/16892908). Associated postcranial elements include parts of the pelvis, limb elements, vertebrae, ribs, scutes, and numerous dermal ossicles. However, much of the postcranial skeleton remains encased in limestone matrix and thus requires preparation before describing it.

Horizon and locality—The limestone concretions containing SAMA P40536 had weathered out of organic-rich marine shales that are lithostratigraphically representative of the Toolebuc Formation. This unit crops out over a vast area west of the township of Boulia in southwestern Queensland (**Figure 1**). The Toolebuc Formation strata around Boulia have long been recognized as abundant sources of vertebrate fossils with documented finds including chimaeroids, lamniform sharks, a diverse range of actinopterygians, ceratodont dipnoans (e.g., Lees, 1986; Rozefelds, 1992; Kemp, 1993; Bartholomai, 2004; Kear, 2007; Wilson et al., 2011; Bartholomai, 2012; Bartholomai, 2015a; Bartholomai, 2015b), marine reptiles incorporating elasmosaurid, polycotylid, and pliosaurid plesiosaurs, ophthalmosaurid ichthyosaurs and protostegid turtles (e.g., Kear, 2003; Kear, 2006; Kear and Lee, 2006; Zammit et al., 2010; Kear and Hamilton-Bruce, 2011; Kear, 2016; Kear et al., 2018), ornithocheiroid pterosaurs (Molnar and Thulborn, 1980; Molnar, 1987; Fletcher and Salisbury, 2010; Kellner et al., 2010, 2011; Pentland and Poropat, 2019), and enantiornithine birds (Molnar, 1986; Chiappe, 1996; Kurochkin and Molnar, 1997; Kear et al., 2003). These assemblages are associated with abundant pelagic cephalopod (ammonites, belemnites, and coleoids) and benthic invertebrate remains (as summarized in Henderson et al., 2000) that indicate a shallow off-shore marine setting subject to poorly oxygenated bottom water conditions (Henderson, 2004; Jiang et al., 2018). Chronostratigraphically, the Toolebuc Formation is correlated with the latest middle–upper Albian *Coptospora paradoxa* spore/pollen and *Pseudoceratium ludbrookiae* dinoflagellate zones (**Figure 1C**; McMinn and Burger, 1986; Moore et al., 1986).

DESCRIPTION

The skull of SAMA P40536 is incomplete and preserves a portion of the palatal region (**Figure 2**). The choanal width is 82 mm, similar to proposed values of 72 mm for *K. ieversi* (measured from Leahey et al., 2015 p. 22), suggesting a potential skull length of ~270 mm and skull width of ~280 mm. The holotype of *K. ieversi* was assumed to be near-mature to mature at the time of death based on its small size and lack of cranial fusion (Molnar, 1996; Leahey et al., 2015). Given the similarity in size, SAMA P40536 may have been of equivalent age.

Although not described herein, a large bony fragment is preserved on the ventral and right lateral surfaces, with the lateral extent unknown due to erosion. The bone is mediolaterally compressed anteriorly and forms a ventrally projecting hook-like process. We tentatively identify this fragment as belonging to the dentary due to its position, ventral to the maxillary tooth row. The paired choanae of SAMA P40536 are separated medially by the posterior portion of the vomer (**Figure 2**). They are crescent-shaped, curving away from the midline posterolaterally, and are slightly wider than they are long. Anteriorly, the vomer, maxillary tooth roots, and maxillary bone impressions form the boundary of both choanae. Typically, the secondary palate separates the choana from the maxillary tooth row (Bourke et al., 2018); however, here, these elements form the choanal boundary due to mediolateral compression of the maxillary tooth row. The palatines form the posterior boundary of the choanae, medially, along with the ectopterygoid, laterally (**Figure 2**). The contribution of ectopterygoid to the choanal boundary suggests that a "posteroventral" secondary palate, which generally braces the palatine against the medial surface of the maxilla, may not have been present (Vickaryous et al., 2004; but see Bourke et al., 2018 for a new interpretation of this palatal structure). The choanae are posteriorly positioned, with their preserved anterior extent roughly in line with the middle of the maxillary tooth row. This condition is similar to that seen in *K. ieversi* but differs from that of ankylosaurids and nodosaurids (Lee, 1996; Godefroit et al., 1999; Carpenter, 2004; Kilbourne and Carpenter, 2005; Leahey et al., 2015; Kinneer et al., 2016).

Facial Bones

Maxilla—The right and left ventromedial surfaces of the maxilla are preserved as impressions on the block; a small bony fragment of the left maxilla is also present along the anterior choanal margin (**Figures 2B,C**). The maxillary impressions form an arcuate contact with the ectopterygoid posteriorly and medially (**Figure 3D**), together forming the lateral and posterolaterally margins of the choanae, respectively. Anteriorly, the impressions enclose the posterior portion of the exposed maxillary tooth roots. Right, and left maxillary tooth rows are partially preserved as impressions of their medial surfaces (**Figure 3C**). The left maxillary tooth row is 82 mm in length, whilst the right is 90 mm. The tooth rows are straight for approximately two-thirds of their length, diverging posteriorly. The final third of the tooth row curves laterally, producing an overall curved tooth row in palatal view. An impression of the alveolar margin occurs on the left side of the block; however, it is not preserved on the right. Approximately 20 tooth impressions are preserved on the right tooth row, with replacement teeth visible dorsal to the impressions of the erupted teeth (**Figure 3C**). There are at least 15 preserved alveolar positions on the left tooth row. As both tooth rows are preserved as incomplete impressions, the total number of teeth within the maxillae is a minimum count.

Palatal Bones

Vomer—The vomer is an anteroposteriorly elongate and mediolaterally compressed bone; becoming dorsoventrally tall, posteriorly (**Figure 4**). Several portions of the nasal septum are missing, but this is likely due to poor mineralization (Witmer and Ridgley, 2008; Leahey et al., 2015). As a result, the dorsal and ventral extents of the vomer are unclear. The ventral nasal keel is partially preserved (**Figure 4C**). As observed in the CT scans, the anterior half of the vomer forms an elongate triangular process

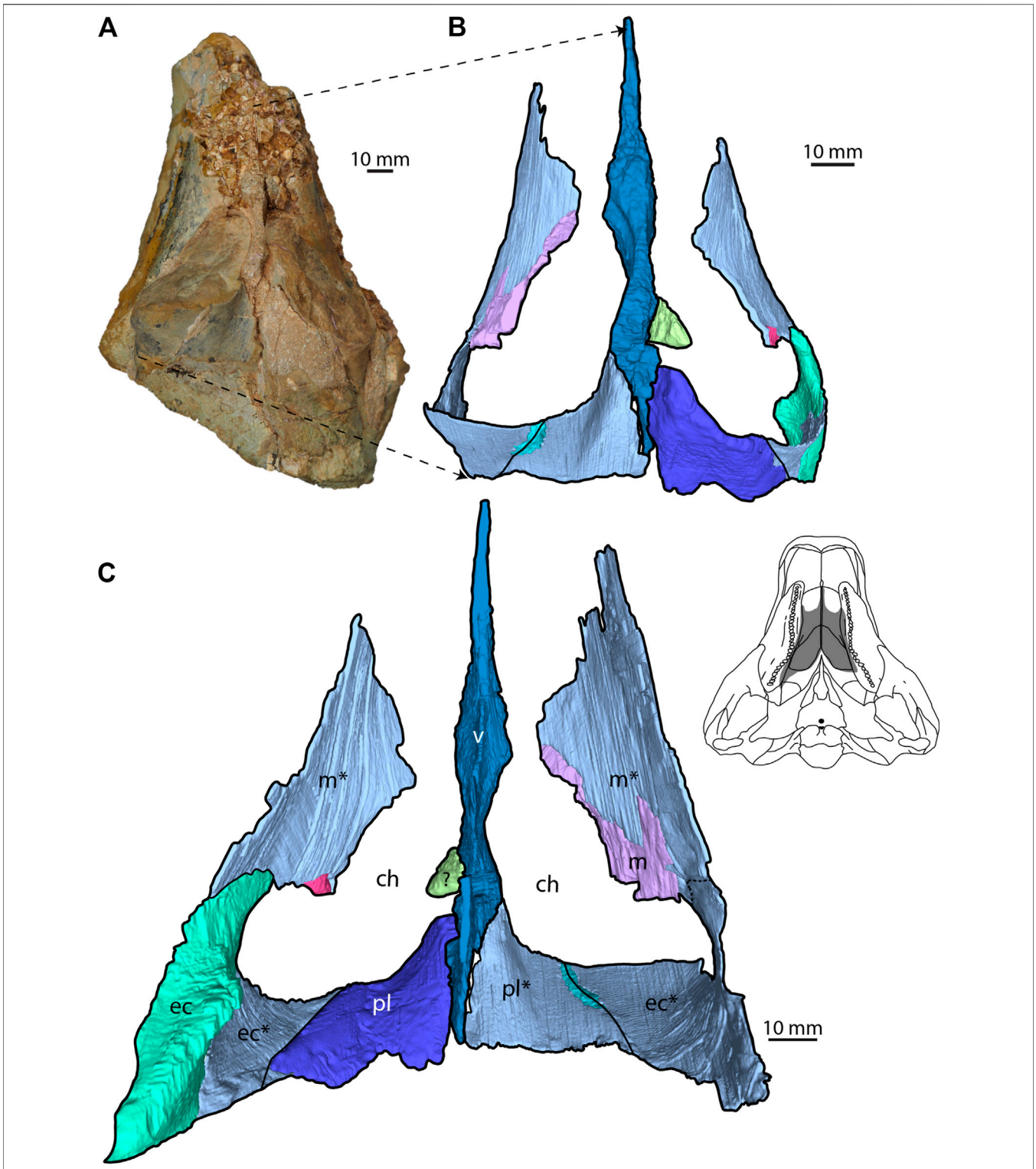

FIGURE 2 | SAMA P40536 palatal region. **(A)** Dorsal view of the specimen. **(B)** Dorsal view of the 3D model. **(C)** Ventral (palatal) view of the 3D model. Skull schematic inset next to C is based on *Kunbarrasaurus ieversi* (modified from Leahey et al., 2015) to show the preserved portion of SAMA P40536 (highlighted in grey). Abbreviations: ch, choana; ec, ectopterygoid; m, maxilla pl, palatine; v, vomer. 3D models of bones based on impressions are denoted with an asterisk (*). See **Supplementary Material S1** for interactive 3D PDF of SAMA P40536.

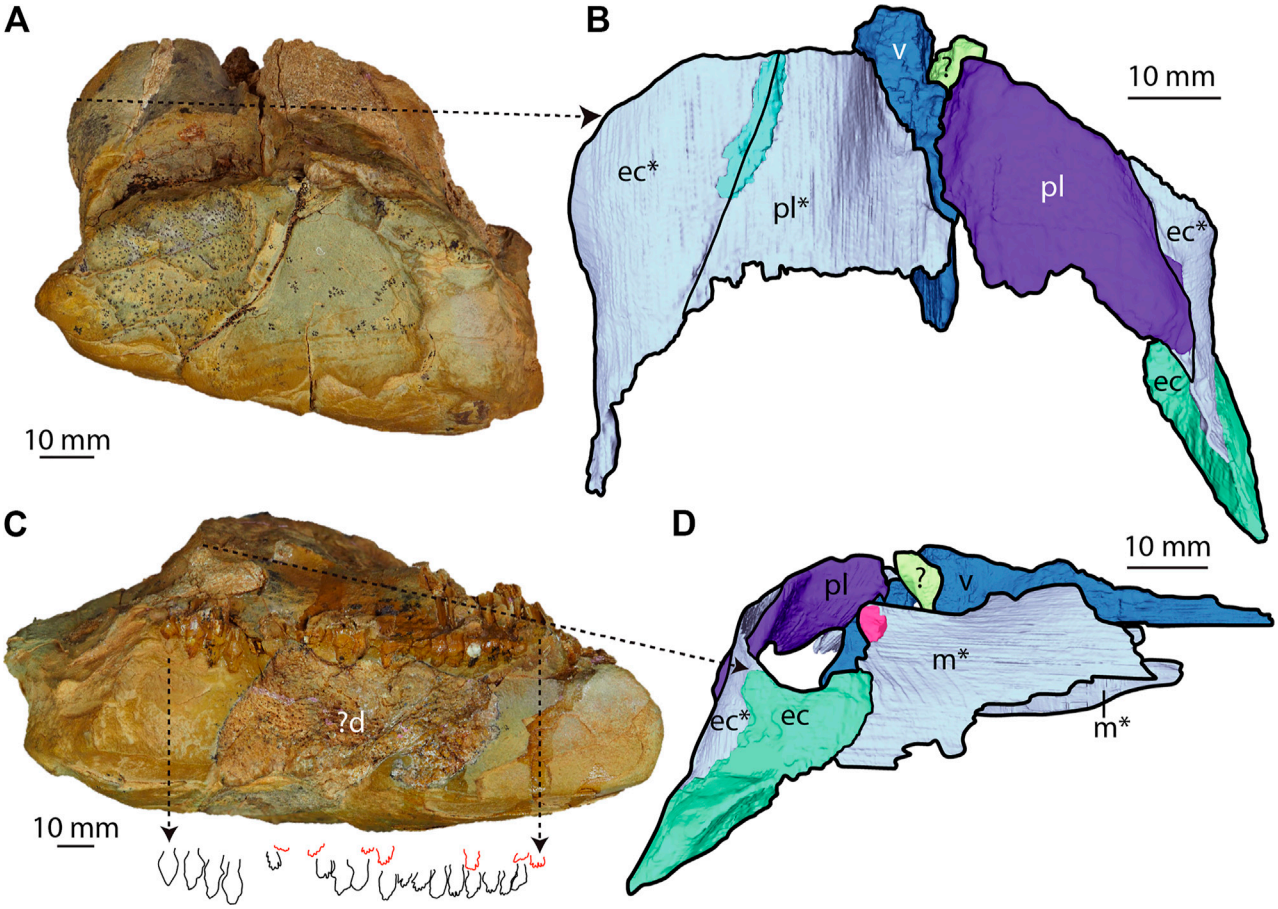

FIGURE 3 | Posterior and right lateral regions of SAMA P40536 **(A,B)** Posterior view. **(A)** Actual specimen. **(B)** 3D reconstruction. **(C,D)** Right lateral view. **(C)** Actual specimen showing the outline of maxillary tooth row impressions, including the functional (black outline) and replacement (red) teeth. Abbreviations: ?d, possibly dentary; ec, ectopterygoid; m, maxilla; pl, palatine; v, vomer. 3D models of bones based on impressions are denoted with an asterisk (*).

that tapers to a point anteriorly (**Figure 4A**). This process is dorsoventrally compressed (**Figure 4C**) with an inverted triangular cross-section and, unlike the posterior half, does not divide the nasal passage. At roughly its mid-point and the mediolateral choanal corner, the vomer mediolaterally expands and is bulbous in dorsal view (**Figure 2C**). A posterodorsally oriented groove is present on the left lateral surface of the expanded region. This groove is not present on the right lateral surface and is a notable asymmetrical feature (**Figures 4C,D**). Posterior to the posterodorsal groove, the vomer expands laterally, resulting in an hourglass shape in dorsal view (**Figures 2B**, **4A**).

Palatines—The palatines form the posteromedial margins of the choanae and are preserved mostly as impressions, with the right preserving a fragment of bone (**Figures 2C**, **3B**). The palatine is a thin, anteroventrally/posterodorsally angled element, similar to other ankylosaurs, such as *Ankylosaurus magniventris* and *Gargoyleosaurus parkpinorum* (Carpenter, 2004; Kilbourne and Carpenter, 2005). Together, the palatines form a U-shaped wall in posterior view that would have separated the palatal and orbital regions, similar to *Pawpawsaurus campbelli* (**Figures 2C**, **3B**; Lee, 1996). Medially, the palatines contact the vomer. Examining the CT data and physical specimen, we cannot confirm if the palatines and vomer are fused (**Figures 2B,C**). The palatines extend posterior to the vomer, suggesting that they contacted each other for part of their length; however, the medial edges of the palatines are missing. Along the posterior margin of the choanae, the palatines contact the ectopterygoid along a straight suture that is angled ventrolaterally in posterior view, similar to *Ankylosaurus* (**Figure 3B**; Carpenter, 2004).

Ectopterygoid—A partial ectopterygoid is preserved as both bone and impression on the right lateral surface of the skull block, and the left ectopterygoid is partially preserved as an impression (**Figures 2C**, **3B**). The ectopterygoid is sub-triangular in mediolateral view (**Figures 5A,B**), curved medially, with a concave dorsal margin forming the choanal posterolateral edge (**Figures 2B**, **5E**). The ectopterygoid contacts the maxilla anteriorly, but the contact would have continued laterally to the ectopterygoid along a scarf joint (**Figure 6**). The ectopterygoid contacts the palatine medially, along the choanal

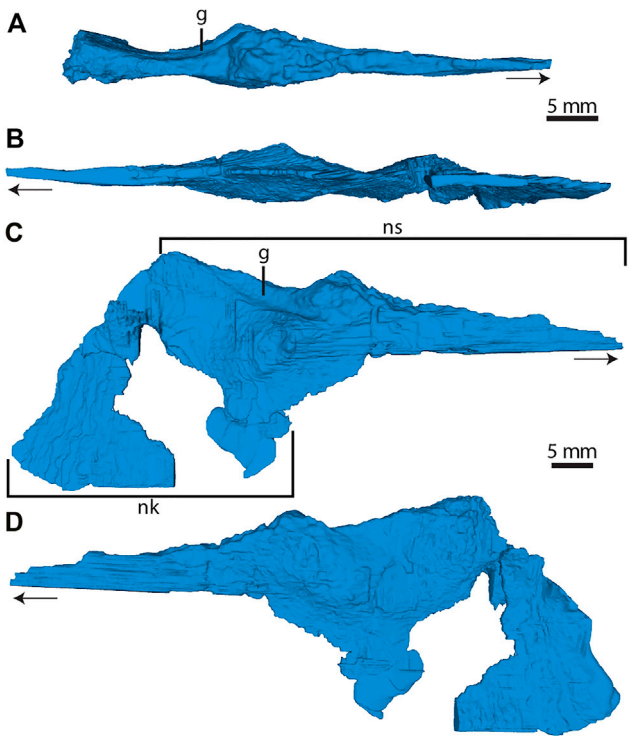

FIGURE 4 | Three-dimensional models of SAMA P40536 vomer. **(A)** Dorsal view. **(B)** Ventral view. **(C)** Right lateral view. **(D)** Left lateral view. Arrow in **(A–D)** points towards anterior. Abbreviations: g, posterodorsal groove; nk, nasal keel; ns, nasal septum.

posterior margin, and forms a straight joint angled ventrolaterally (**Figure 6**). The posteroventral corner is drawn out into a wedged-shaped process (as preserved) buttressed medially along its length (**Figure 5**).

TABLE 1 | Measurements (in mm) of all preserved ankylosaur teeth in SAMA P40536.

Tooth id	AB	MD	LL	RL	R/L
In-situ tooth	5.4	4.6	2.0	—	L
Yellow	5.1	4.6	1.9	16	R
Red	6	4.5	1.6	14.6	L
Pink	—	—	—	15	—
Blue	4.3	4.3	1.6	—	L
Lime green	5.2	3.9	1.2	—	L
Green	—	3.7	2	13.4	—
Salmon	5.3	4.5	2.1	15.5	?L

Abbreviations: AB, apicobasal height; MD, mesiodistal length; LL, labiolingual width; RL, root length; R/L, right or left jaw. Tooth id is based on the name and color used in the 3D models as seen in ***Supplementary Materials S1, S2****.*

Dentition

Eight isolated teeth are identified from the CT scans: one *in situ* left maxillary tooth crown and seven isolated teeth with roots of unknown position found "floating" within the matrix (**Table 1**; **Supplementary Materials S1, S2**). Of these, the *in situ* crown provides the best resolution and the basis for the following description (**Figures 7H–J**). The crown is asymmetrical in labial view and is labiolingually compressed (**Figures 7I,J**). The apex corresponds to the primary ridge/denticle (sensu Bell et al., 2018b) and is distally offset. The primary denticle is marginally larger than the remaining denticles and bears a shallow, mesiodistally oriented, and grooved wear facet on the apex. Two denticles are present distal to the primary denticle and three mesially. Denticles are apically pointed and curved away from the central tooth axis, giving the crown a fan-shaped appearance. Apicobasal grooves (or sulci) between denticles extend basally but do not appear to have reached the cingulum (**Figure 7**; the cingulum itself is only preserved on the more

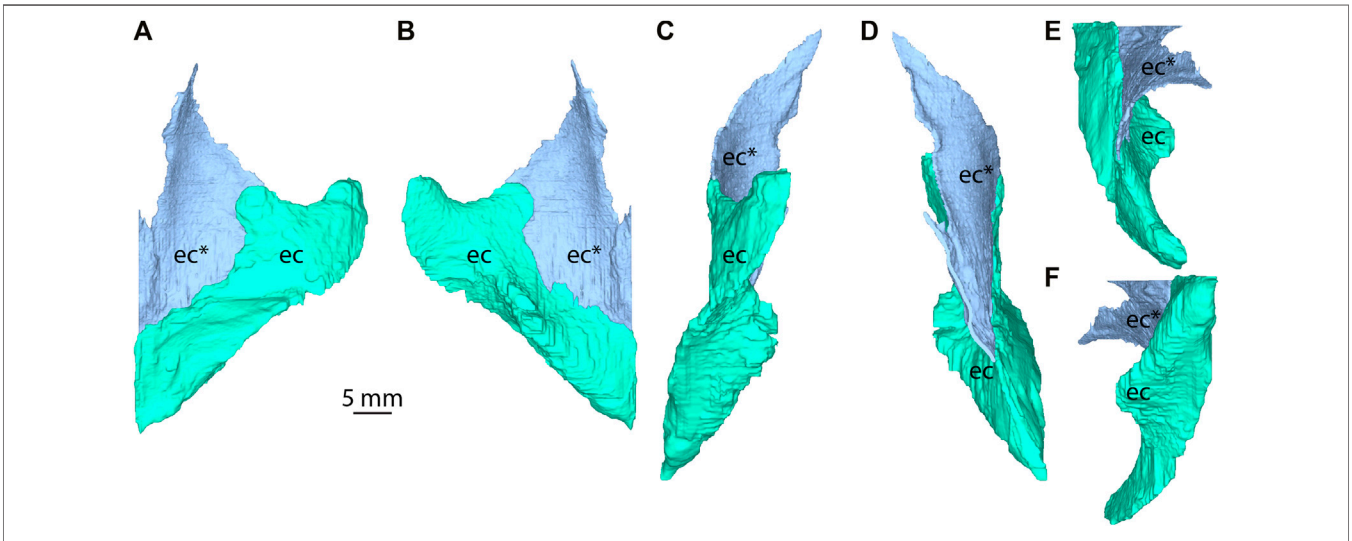

FIGURE 5 | Three-dimensional models of SAMA P40536 right ectopterygoid. **(A)** Lateral view. **(B)** Medial view. **(C)** Anterior view. **(D)** Posterior view. **(E)** Dorsal view. **(F)** Ventral view. Abbreviations: ec, ectopterygoid. 3D models of bones based on impressions are denoted with an asterisk (*).

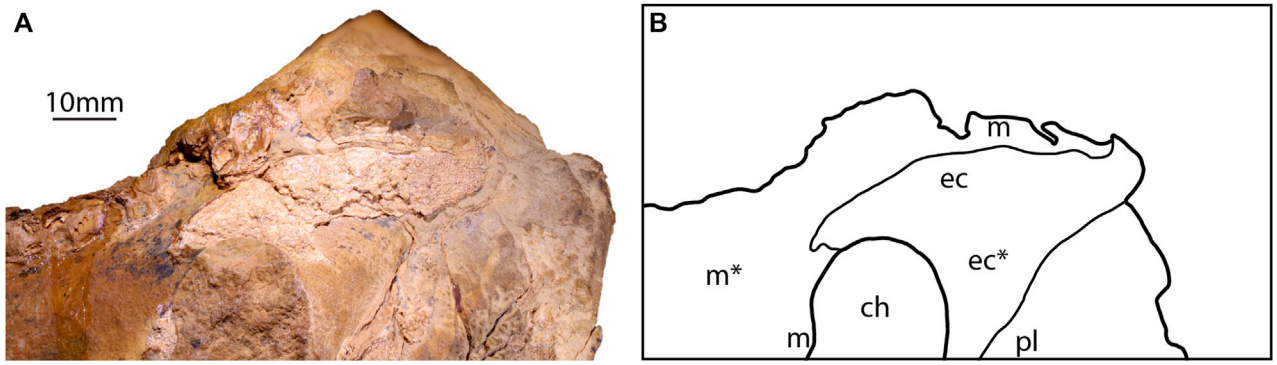

FIGURE 6 | Scarf joint between the right ectopterygoid and right maxilla of SAMA P40536. **(A)** Dorsolateral view of the physical specimen. **(B)** A line drawing showing the contact between the ectopterygoid and the maxilla. Abbreviations: ch, choanae; ec, ectopterygoid; m, maxilla; pl, palatine. Regions based on impressions are denoted with an asterisk (*).

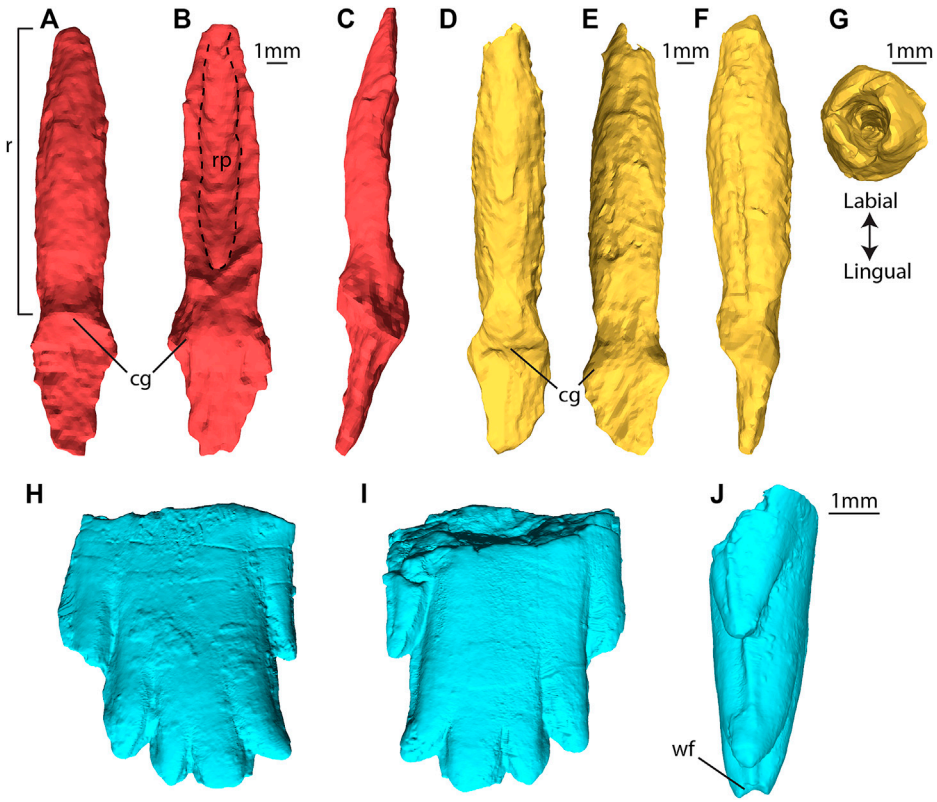

FIGURE 7 | Three-dimensional models of select SAMA P40536 maxillary teeth. **(A–C)** *Ex situ* maxillary tooth in **(A)** lingual, **(B)** labial, and **(C)** distal views. **(D–G)** *Ex situ* maxillary tooth in **(D)** lingual, **(E)** labial, **(F)** mesial, and **(G)** basal views. **(H–J)** *In situ* (MicroCT) posterior maxillary tooth in **(H)** lingual, **(I)** labial, and **(J)** apical-mesial views. **(A–G)** Preserved within the block, extracted virtually. **(H–J)** Was manually prepared and subsequently, micro-CT scanned. Abbreviations: cg, cingula; r, root; rp, resorption pit (outlined in a dashed line in B); wf, wear facet. Tooth colors correspond to those in **Table 1** and **Supplementary Material S1** (*ex situ*) and **Supplementary Material S2** (*in situ*).

complete isolated teeth; see above). Individual denticles are difficult to identify on the isolated teeth due to the low resolution of the CT scans; however, small bumps on the crowns suggest five to seven denticles (including the primary denticle) were present per tooth (**Figures 7A,E**).

The low denticle count is similar to *K. ieversi* and other nodosaurids but differs from the approximately 8–12 denticles per tooth seen in the upper Strzelecki group teeth (Molnar, 1996; Barrett et al., 2010; Leahey et al., 2015). The *in situ* crown is broken basally, and the presence of cingula are unknown;

however, cingula are present on five isolated teeth. The lingual cingulum is prominent, forming a bulbous shelf, whereas the labial cingulum is less prominent and positioned apically (**Figures 7A–F**). Five teeth preserve large roots, two to three times taller than the crowns (**Table 1**), separated by a constriction. Roots are straight, bullet-shaped, and circular in cross-section, similar to other Australian ankylosaurian teeth (**Figure 7G**; Molnar, 1996; Barrett et al., 2010; Leahey and Salisbury, 2013). Two isolated teeth have partially resorbed roots, as the labial surface is either partially or completely missing (**Figure 7B**), suggesting root resorption proceeded in a labial–lingual direction. All tooth impressions from the right maxilla have prominent lingual cingula. Consistent with the *in situ* maxillary crown, tooth impressions have anywhere from five to seven denticles. Crowns of the 16 mesial-most teeth are fan-shaped, whereas the four distal-most teeth are more pointed (**Figure 3C**). The preserved crown impressions range from 4 to 6 mm wide and 5–8 mm long.

TABLE 2 | Characters coded for the phylogeny of SAMA P40536.

Character	SAMA P40536 character states
28	1-Maxillary tooth row is medially convex
31	0-Caudoventral secondary palate absent
88	1-Cingulum on maxillary and/or dentary teeth is present
89	0-Maxillary and/or dentary tooth crown shape is pointed
90	0-Maxillary and/or dentary tooth denticles <13 denticles
178/190*	1-The choanae are posteriorly placed approx. mid-way along the tooth row
179*	0-Tooth crowns are asymmetric
180*	1-Tooth crown striations extend to cingulum
181*	1-Tooth crown striations are confluent with denticles

Information on characters 1–177 is available in Arbour and Currie (2016), whilst information on characters 178–189 are available in Soto-Acuña et al. (2021, ***Supplementary Figure S6****). Character 178/190 on the choanae is discussed within text. All characters denoted with an asterisks (*) are only in the modified Soto-Acuña et al. (2021) matrix. See matrices in* ***Supplementary Material S3*** *for all character codes.*

PHYLOGENETIC ANALYSIS

Methods

SAMA P40536 was scored into two phylogenetic datasets (**Supplementary Material S3**): Arbour and Currie (2016) (Modified from Thompson et al., 2012; Arbour and Currie, 2013; Arbour et al., 2014a; Arbour et al., 2014b) and Soto-Acuña et al. (2021) (Modified from Arbour and Currie, 2016; Arbour et al., 2016). The Arbour and Currie (2016) matrix consists of 178 characters and 45 ingroup taxa, including SAMA P40536 (scores provided in **Table 2**) and the non-ankylosaurian outgroup taxa *Lesothosaurus diagnosticus*, *Sceliosaurus harrisonii*, and *Huayangosaurus taibaii*. In this matrix, we updated the terminal taxon designation from *Minmi* sp. to *Kunbarrasaurus ieversi*, and "*Zhejiangosaurus lishuiensis*" replaced the incorrectly identified "*Zhejiangosaurus luoyangensis*" (Lü et al., 2007; Leahey et al., 2015). The Soto-Acuña et al. (2021) matrix consists of 190 characters and 66 ingroup taxa, including SAMA P40536 (scores provided in **Table 2**) and the non-ankylosaurian outgroup taxa *Lesothosaurus diagnosticus*, *Scelidosaurus harrisonii*, and members of Stegosauria (*Huayangosaurus taibaii*, *Paranthodon africanus*, and *Stegosaurus stenops*). Here, we updated the terminal taxon designation from *Sauropelta edwardsi* to *Sauropelta edwardsorum*, and "Argentinian ankylosaur" replaced the "Salitral Moreno ankylosaur" for consistency between matrices.

To incorporate additional palatal variations noted in SAMA P40536, *K. ieversi*, and other ankylosaurians, we added a new character (178 in Arbour and Currie, 2016; and 190 in Soto-Acuña et al., 2021) that describes the position of the choanae within the palate relative to the maxillary tooth row: choanae with their anterior margins inline or within the anterior third of the maxillary tooth row (178/190:0); choanae posteriorly situated with their anterior margins at least mid-way along the tooth row (178/190:1). Ankylosaurians were scored from the literature (Eaton Jr, 1960; Sereno and Zhimin, 1992; Lee, 1996; Godefroit et al., 1999; Carpenter et al., 2001a, 2008, 2011; Vickaryous et al., 2001; Hill et al., 2003; Carpenter, 2004; Kilbourne and Carpenter, 2005; Parsons and Parsons, 2009; Arbour and Currie, 2013; Arbour et al., 2014a; Leahey et al., 2015; Kinneer et al., 2016; Arbour and Evans, 2017; Yang et al., 2017; Bourke et al., 2018; Paulina-Carabajal et al., 2018; Wiersma and Irmis, 2018; Norman, 2020; Park et al., 2020); however, we could not adequately code the outgroup taxon *Huayangosaurus taibaii* because the condition of its choanae is unknown. Character polarity was therefore determined from *Hesperosaurus mjosi* (Maidment et al., 2018) and a 3D cranial model of *Stegosaurus armatus* (specimen number; UMNH VPC 44, sketchfab. com/ivlpaleontology), which preserve the choanae approximately in line with the anterior-most maxillary tooth (Sereno and Zhimin, 1992; Carpenter et al., 2001b; Chengkai et al., 2007; Mateus et al., 2009). The anterior extent of the choanae in *Lesothosaurus diagnosticus* is likewise not directly observable. Nonetheless, the maxillae are mediolaterally compressed and unlikely to have formed a bony palate as in many ankylosaurs (Porro et al., 2015). Consequently, we interpret the anterior margins of the choana as probably being anteriorly placed. Finally, the choanae of *Scelidosaurus harrisonii* end anteriorly relative to the anterior-most maxillary tooth (Norman, 2020). Character 31 was recoded as "?" for *K. ieversi* in both matrices because the placement of the ectopterygoid cannot be adequately interpreted from the physical specimen or 3D tomographic renderings (Leahey et al., 2015). Moreover, given the absence of a "caudoventral" secondary palate in SAMA P40536, it is doubtful that such as structure was present in *K. ieversi*.

The updated character-taxon matrices were compiled using *Mesquite* version 3.61 (Maddison and Maddison, 2019) and analyzed in *TNT* version 1.5 (Goloboff and Catalano, 2016). All characters were assumed unordered and of equal weight, with *Lesothosaurus diagnosticus* designated the most distant outgroup taxon in both matrices. Both matrices were subjected to a phylogenetic analysis involving 1,000 replicates of a "traditional" search using random addition sequence starting trees and the Tree Bisection Reconnection (TBR) branch swapping algorithm. Following the initial search, we performed another round of branch swapping on the set of most parsimonious trees (MPTs) using TBR to more fully explore the tree space. We used iterative PCR to identify wildcard taxa that could be pruned to improve

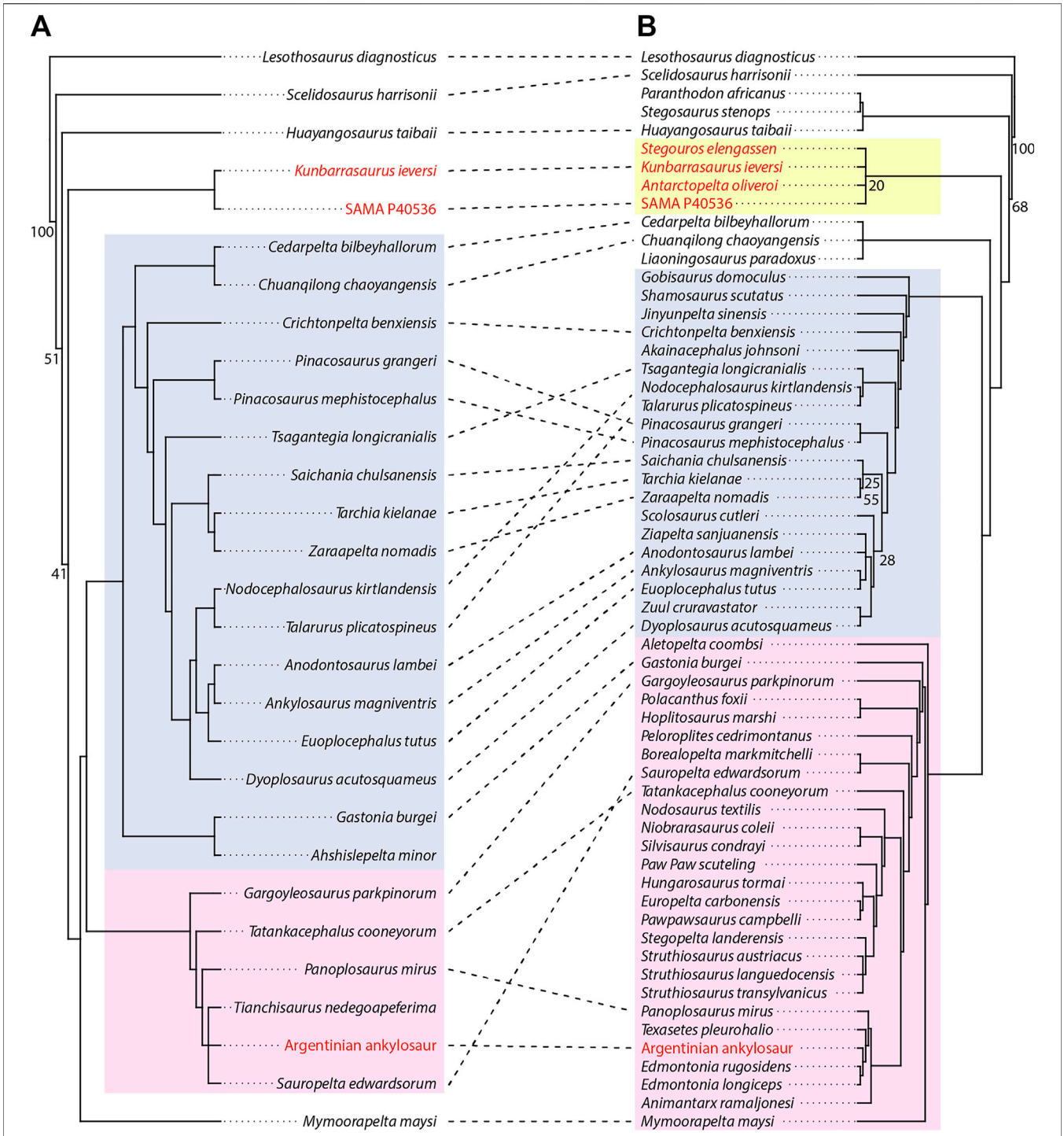

FIGURE 8 | Results of the phylogenetic analyses. **(A)** Reduced strict consensus of 1,630 MPTs of 423 steps (CI: 0.536, RI: 0.704, RC: 0.377) recovered after inclusion of SAMA P40536 into the character-taxon matrix of Arbour and Currie (2016), **(B)** Reduced strict consensus of the 20 MPTs of 696 steps (CI: 0.359, RI: 0.653, RC: 0.234) recovered after inclusion of SAMA P40536 into the character-taxon matrix of Soto-Acuña et al. (2021). Node labels indicate GC bootstrap support values above 20. Bootstrap values for all nodes are provided in **Supplementary Material S3 (Figures S3.1 and S3.2)**. All Gondwanan taxa are highlighted in red. The extent of Parankylosauria is highlighted in yellow, Ankylosauridae in blue, and Nodosauridae in pink.

resolution in the strict consensus of the final set of MPTs (Pol and Escapa, 2009), while retaining SAMA P40536. Nodal supports for the resulting reduced strict consensus tree from each matrix were calculated from 1,000 bootstrap resampling replicates using the same initial "traditional" tree search strategy. Clade frequencies were summarised using the Groups present/Contradicted (GC) metric.

Results

The phylogenetic analysis of Arbour and Currie (2016) returned 1,630 MPTs of 423 steps [Consistency Index (CI): 0.536, Retention Index (RI): 0.704, Rescaled Consistency Index (RC): 0.377] from the initial tree search, and over 10,000 additional trees of equal length after another round of branch swapping. Sixteen wildcard taxa were identified for removal by iterative PCR: *Aletopelta coombsi, Antarctopelta oliveroi, Bissektipelta archibaldi*, *Dongyangopelta yangyanensis, Glyptodontopelta mimus, Gobisaurus domoculus, Liaoningosaurus paradoxus, Minmi paravertebra*, *Pawpawsaurus campbelli, Sauroplites scutiger, Scolosaurus cutleri, Shamosaurus scutatus, Stegopelta landerensis, Taohelong jinchengensis, Zhejiangosaurus lishuiensis, and Zipaleta sanjuanensis*. The reduced strict consensus tree is almost completely resolved (**Figure 8A**); Ankylosauridae is fully resolved, whilst Nodosauridae contains one polytomy (*Sauropelta edwardsorum, Tianchisaurus nedegoapeferima,* and the Argentinian ankylosaur). SAMA P40536 was recovered as the sister of *K. ieversi*, which together form the sister clade to *Mymoorapelta maysi* + Ankylosauridae + Nodosauridae (**Figure 8A**). *Kunbarrasaurus ieversi* and SAMA P40536 share two autapomorphies: the maxillary tooth row is medially convex (28:1), and the choanae are posteriorly placed approximately mid-way along the maxillary tooth row (178:1). As *M. paravertebra* was removed by IterPCR, the relationship with SAMA P40536 is currently unknown; however, when the analysis was run with *M. paravertebra* included, the tree collapsed into a large polytomy (results not included).

The initial search of Soto-Acuña et al. (2021) returned 20 MPTs of 693 steps (CI: 0.359, RI: 0.653, RC: 0.234). More than 10,000 trees of equal length were found after another round of branch swapping. Seven wildcard taxa were identified for removal by iterative PCR: *Ahshislepelta minor*, *Denversaurus schlessmani*, *Donyangopelta yangyanensis*, *Hylaeosaurus armatus*, *Sauroplites scutiger*, *Taohelong jinchengensis*, and *Zhejiangosaurus lishuiensis*. Both Ankylosauridae and Nodosauridae are well resolved in the resulting reduced strict consensus tree (**Figure 8B**), each containing one polytomy (*Ziapelta sanjuanensis* and *Anodontosaurus lambei*, and all three *Struthiosaurus*, respectively). Parankylosauria is monophyletic but unresolved, recovered as the sister-taxon to Ankylosauridae, Nodosauridae, and a clade formed by *Cedarpelta bilbeyhallorum*, *Chuanqilong chaoyangensis*, and *Liaoningosaurus paradoxus*. Parankylosauria contains *Stegouros elengassen*, *K. ieversi*, and *A. oliveroi*, as in Soto-Acuña et al. (2021), along with SAMA P40536.

DISCUSSION

Comparisons with *Kunbarrasaurus ieversi*

SAMA P40536 shares five features with *Kunbarrasaurus ieversi*: a sinuous maxillary tooth row, posteriorly placed choanae, asymmetric tooth crowns, and tooth crown striations that are both confluent with the denticles and extend to the cingulum (**Table 2** for clarification on matrix assignment). In addition, SAMA P40536 and *K. ieversi* share teeth with low denticle counts, cylindrical tooth roots, and both lingual and labial cingula (Molnar, 1996). Unfortunately, none of the *K. ieversi* autapomorphies identified on the holotype (QM F18101; Leahey et al., 2015) are preserved in SAMA P40536, precluding unambiguous referral. Nevertheless, their dental and choanal similarities are sufficient to recover both specimens as sister-taxa (**Figure 8A**) and within Parankylosauria with the added tooth characters (**Figure 8B**). Combined with their spatiotemporal proximity (**Figure 9**), we provisionally refer SAMA P40536 to cf. *Kunbarrasaurus* sp. pending further preparation and description of the postcranial skeletons.

Although our taxonomic assignment is tentative, the palatal osteology of SAMA P40536 fills anatomical gaps not observable in QM F18101 (Leahey et al., 2015). For example, the palatines of SAMA P40536 are vertically positioned and separate the palatal and orbital regions. Although the posterior extent of the palatines is not preserved, vertical sutures along the posterior margins of the choanae represent the contacts between the palatines and the ectopterygoids (**Figures 3A,B**). This arrangement indicates that the ectopterygoid forms the posterolateral margin of the choana, as in *Edmontonia longiceps* (Vickaryous et al., 2004). Furthermore, the palatines did not contact the maxillae along the choanal margin as reconstructed by (Leahey et al., 2015). The ectopterygoid contacts are unknown in *K. ieversi* due to poor preservation and encasing matrix (Leahey et al., 2015) but differ from the interpretation of (Leahey et al., 2015, p. 22, **Figure 6**), who placed the ectopterygoid more posteriorly between the maxilla and pterygoids.

Implications of Choanal Variation in Ankylosaurs

The palatal choanae form part of the nasal passages and are the boundary between the internal cranial nasal passages and the buccal region (Bourke et al., 2018). Therefore, it may be expected that choanal variations reflect the complexities of ankylosaurian nasal passages, such as mineralised soft tissue creating convoluted nasal passages and the paranasal sinus system formed by an extensive set of air sacs surrounding the nasal airways. (Brown and Kaisen, 1908; Vickaryous et al., 2004; Vickaryous, 2006; Witmer and Ridgley, 2008; Leahey et al., 2015; Paulina-Carabajal et al., 2016; Bourke et al., 2018). Surprisingly, the palate remains an anatomically under-sampled component of ankylosaur phylogenies. Indeed, only five of the 178 and 190 characters employed in both matrices capture palatal morphologies. We found notable variation in the relative placement of the choana within the palate. The majority of ankylosaurians display choanae that span most of the palatal region, and the anterior choanal margins are either in line with the anterior-most maxillary tooth (e.g., *Pawpawsaurus campbelli*; Paulina-Carabajal et al., 2016 p. 5) or within the anterior third of the tooth row (e.g., *Ankylosaurus magniventris*; Carpenter, 2004). As we used the literature to code most ankylosaurian taxa, we simplified the previous conditions into a single character relative to the outgroup (Sereno and Zhimin, 1992; Porro et al., 2015; Maidment et al., 2018; Norman, 2020), indicating that anteriorly placed choanae are primitive for ankylosaurs. By contrast, SAMA P40536 and *K. ieversi* exhibit a derived condition whereby the choanae are relatively posterior within the palate. The other parankylosaurian *Stegouros ellengassen* may also exhibit this derived condition, as the secondary palate that marks the anterior extent of the choanae extends posteriorly to approximately the mid-point of the preserved tooth row (Soto-Acuña et al., 2021). Unfortunately, the maxillary

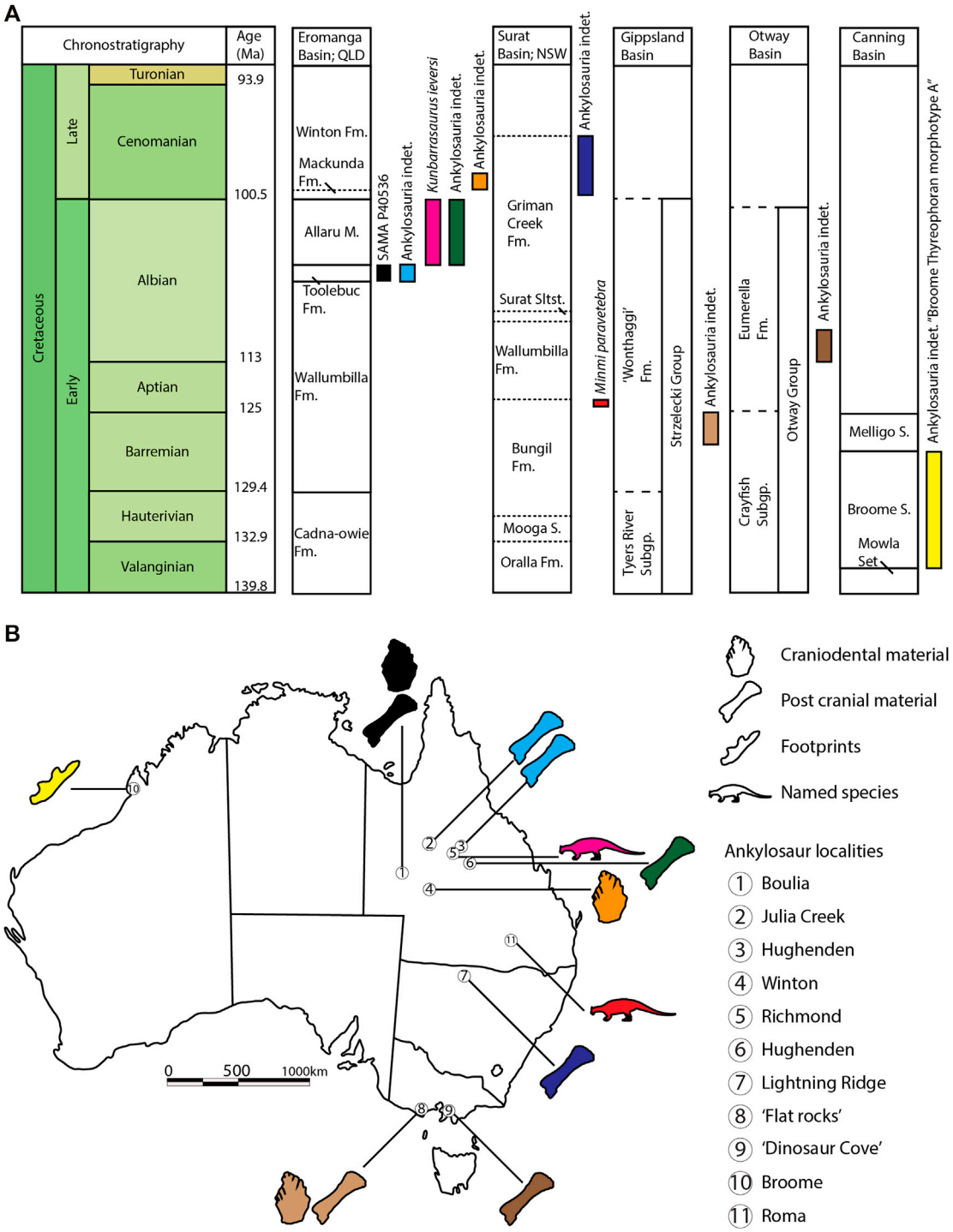

FIGURE 9 | Biostratigraphic and palaeobiogeographic context of mid-Cretaceous Australian ankylosaurs. **(A)** Simple biostratigraphy of ankylosaurs from the Surat Basin (Molnar, 1980; Bell et al., 2018a), Eromanga Basin (Molnar, 1996; Leahey and Salisbury, 2013; Leahey et al., 2015), Gippsland and Otway Basins (Barrett et al., 2010), and Canning Basin (Salisbury et al., 2016). Chronostratigraphy data was compiled from Salisbury et al. (2016); Bell et al. (2019); Wagstaff et al. (2020); and Cooling et al. (2021). Dashed lines represent geological unconformities, whilst dotted lines represent gradational boundaries **(B)** Palaeobiogeography and the fossil record of Australian ankylosaurs from 11 sites, modified from Leahey et al. (2015). Ankylosaur silhouette generated by Jagged Fang Designs and reused under Creative Commons licenses: Public Domain Dedication 1.0.

tooth row is incomplete posteriorly and so we cannot confirm its condition at this time, and it was coded as "?". The derived condition stabilizes SAMA P40536 within both trees but otherwise does not dramatically affect the phylogenetic placements of other ankylosaurians. Without this character, the trees collapse into a large polytomy with virtually no basal resolution (results not provided). It is worth noting that if future postcranial observations of SAMA P40536 support an assignment to *K. ieversi*, this character may represent a new autapomorphy for *K. ieversi*.

Presently, only the ankylosaurids *Cedarpelta bilbeyhallorum*, and *Gobisaurus domoculus* (Vickaryous et al., 2001; Carpenter et al., 2008) exhibit posteriorly positioned choanae comparable to *K. ieversi* (Leahey et al., 2015) and SAMA P40536. The ankylosaurid *Akainacephalus johnsoni* and the nodosaurid *Panoplosaurus mirus* show the most extreme condition, whereby the anterior choanal margins are approximately in line with the posterior-most maxillary tooth (Bourke et al., 2018; Wiersma and Irmis, 2018). These occurrences suggest that posteriorly located choanae evolved independently at least four times: once before the Nodosauridae + Ankylosauridae split, once in nodosaurids, and at least twice in ankylosaurids. Note that there is currently no resolution on the relationships of *C. bilbeyhallorum* and *G. domoculus* in Arbour and Currie (2016) and that our safe taxonomic reduction analysis of their matrix excluded *G. domoculus*. However, our analysis of the Soto-Acuña et al. (2021) matrix places *C. bilbeyhallorum* outside of Ankylosauridae + Nodosauridae (**Figure 8B**), which would incur a more complex evolutionary path for the character. However, we refrain from over interpreting this tree given its labile nature (See next **Section**).

The phylogenetic placement of SAMA P40536 as an early-branching ankylosaurian has implications for interpreting choanal and palatal variations in ankylosaurs. The bones forming the choanal margins are often difficult to discern due to a tightly sutured or fused nature. The preserved palatal bones of SAMA P40536 are not fused, and contacts are visible. The choanal margins are formed by four bones, the maxilla, vomer, ectopterygoid, and palatines (**Figure 2**). Given that the ectopterygoid contributes to the choanal margin, the palatines were excluded from contacting the maxilla, suggesting that SAMA P40536 did not have a "posteroventral" secondary palate (Vickaryous et al., 2004) or *lamina transversa* (Bourke et al., 2018); these contacts are unknown in *K. ieversi* (Leahey et al., 2015). Therefore, our results indicate that the ankylosaurian *lamina transversa* evolved later in ankylosaur evolution, perhaps due to modifications to the nasal passages (Bourke et al., 2018). Functionally, the *lamina transversa* separates the olfactory and nasal regions and is associated with a heightened sense of smell (Bourke et al., 2018). Therefore, its absence in SAMA P40536 suggests that a more basic sense of smell was primitive for ankylosaurians.

Implications for Australian Ankylosaur Diversity

Australia has the largest abundance of Gondwanan ankylosaurs and species-level diversity documented from the mid-Cretaceous (**Figure 9**; Molnar, 2001; Barrett et al., 2010; Leahey and Salisbury, 2013; Leahey et al., 2015; Salisbury et al., 2016; Bell et al., 2018a). Occurrences include ankylosaur footprints from the Valanginian–Barremian Broome Sandstone of Western Australia (Salisbury et al., 2016), isolated skeletal elements from the uppermost Barremian–lower Aptian "Wonthaggi formation" strata of the upper Strzelecki Group in Victoria, *Minmi paravertebra* from the lower Aptian Bungil Formation of Queensland, *Kunbarrasaurus ieversi* from the upper Albian Allaru Mudstone of Queensland, and other indeterminate bones and teeth from the uppermost Albian–lower Cenomanian Mackunda and Griman Creek formations of Queensland and New South Wales, respectively (Molnar, 2001; Barrett et al., 2010; Leahey and Salisbury, 2013; Leahey et al., 2015; Bell et al., 2018a). Historically, all Australian ankylosaur fossils were referred to the genus *Minmi* (Molnar, 1980, 1996); however, the re-classification of *K. ieversi* (previously *Minmi* sp.; Leahey et al., 2015) as a separate genus and species implicates greater intra-clade diversity. Our attribution of SAMA P40536 to cf. *Kunbarrasaurus* sp. further extends the stratigraphical range of this taxon into the lower–upper Albian and evinces a novel sampling occurrence some ~550 km to the SW of other earlier discoveries.

Previous phylogenies treated *K. ieversi* (QM F18101) and *M. paravertebra* (QM F10329) as a generic hypodigm, recovering it as either a sister to all other ankylosaurians (Kirkland, 1998; Carpenter, 2001) or ankylosaurids (Sereno, 1999; Hill et al., 2003; Vickaryous et al., 2004; Ősi, 2005; Burns et al., 2011; Thompson et al., 2012). However, *K. ieversi* is now considered an early-branching ankylosaurian outside of both Ankylosauridae and Nodosauridae (Arbour and Currie, 2016). Recently, the discovery of *Stegouros ellengassen* introduced a new phylogenetic hypothesis, whereby *K. ieversi*, *S. ellengassen*, and *Antarctopelta oliveroi* form a Gondwanan ankylosaur clade, Parankylosauria, which would have diverged before the Ankylosauridae + Nodosauridae split (Soto-Acuña et al., 2021). In testing the phylogenetic position of SAMA P40536, we were unable to reproduce the same tree from Soto-Acuña et al. (2021), even when the aforementioned specimen was removed. Our replication attempt produced 20 MPTs and contained several differences in the strict consensus, such as a polytomy outside of Ankylosauridae + Nodosauridae containing *Chuanqilong chaoyangensis*, *Lianingosaurus paradoxus* and *Cedarpelta bilbeyhallorum*, and slightly better resolution within Ankylosauridae and Nodosauridae (**Supplementary Material S3**; **Supplementary Figure S3.2**). Furthermore, an additional round of branch swapping on the initial 20 MPTs produced over 10,000 MPTs with considerably reduced resolution in the strict consensus. For instance, there was no clear split between Ankylosauridae and Nodosauridae and most ingroup taxa were reduced to a polytomy (**Supplementary Material S3**; **Supplementary Figure S3.3**). The reason for the difference in phylogenetic hypothesis observed in our replication of Soto-Acuña et al. (2021) is unclear; however, it likely stems from the overall poorly supported nature of ankylosaur phylogenetics. Fortunately, these broader differences had no effect on the phylogenetic placement of SAMA P40536 and Parankylosauria was nonetheless recovered in all analyses, supporting the existence of an early-branching, exclusively Gondwanan ankylosaurian clade. Given the placement of SAMA P40536 as

the sister taxon of *K. ieversi* in the Arbour and Currie (2016) phylogeny, it is not surprising that it is also occurs within Parankylosauria. All four terminal units share four dental features: asymmetric tooth crowns, striations confluent with the denticles and extend to the cingula, and cingulum present on either maxillary or dentary teeth. Of note, the first three features are also present in the Argentinian ankylosaur (Coria and Salgado, 2001), although current hypotheses place it deep within Nodosauridae (**Figure 8**).

Previous studies hypothesized that Australian ankylosaurians evolved independently from the Late Cretaceous ankylosaurs found elsewhere in Gondwana (i.e., *A. oliveroi* and the Argentinian ankylosaur), which were previously considered to be more closely related to Laurasian nodosaurids (**Figure 8A**; Coria and Salgado, 2001; Salgado and Gasparini, 2006; Arbour and Currie, 2016; Arbour et al., 2016). However, the proposed existence of Parankylosauria suggests that most Gondwanan ankylosaurs are more closely related to each other than to those found elsewhere (Soto-Acuña et al., 2021). The only current exception is the Argentinian ankylosaur, a nodosaurid (**Figure 8**) that appeared in Gondwana following dispersal events from Laramidia during the Campanian–Maastrichtian, a pattern also observed among hadrosaurids and titanosaurs (Brett-Surman, 1979; Coria and Salgado, 2001; Prieto-Márquez, 2010; Arbour and Currie, 2016; Ibiricu et al., 2021). Given the mid–upper Albian ages of Australian ankylosaurs, the Gondwanan dispersal of Parankylosauria considerably predated those of the latest Cretaceous (Arbour and Currie, 2016; Kubo, 2020; Soto-Acuña et al., 2021). Interestingly, the recent identification of the putative ankylsoaur *Spicomellus afer* from the mid-Jurassic of Morocco (Maidment et al., 2021) hints at an initial, more ancient global diversification of Ankylosauria (Gibbons et al., 2013; Arbour and Currie, 2016; Arbour et al., 2016; Maidment et al., 2021; Soto-Acuña et al., 2021).

CONCLUSION

Here, we described the second Australian ankylosaur cranium and the first ankylosaurian remains from the Toolebuc Formation. Its conferral to *Kunbarrasaurus* is based on palatal and dental similarities. However, without extensive overlapping anatomy, an unambiguous referral is currently not possible. Nonetheless, several skull elements unknown in the holotype of *K. iveresi* can be inferred by SAMA P40536, notably the position and morphology of the palatines and their relation to the ectopterygoids. The future examination of SAMA P40536's postcranial skeleton with those of *K. ieversi* and *Minmi paravertebra* will elucidate its taxonomic affinities, further testing the phylogenetic affinities of Australian and Gondwanan ankylosaurs. The exploration of palatal morphology uncovered a new phylogenetic character, and highlights the importance of this anatomical region in resolving ankylosaur phylogenetic relationships.

DATA AVAILABILITY STATEMENT

Raw data and 3D models are available at MorphoSource (ark:/87602/m4/392687): https://www.morphosource.org/projects/000392635?locale=en. **Supplementary Material** (3D PDF) S1 and S2 are available at Figshare: https://figshare.com/articles/figure/3D_PDF_of_SAMA_P40536-_Frauenfelder_et_al_/16892908.

AUTHOR CONTRIBUTIONS

TGF and NEC conceived and designed the study, and prepared figures or tables. TGF, PRB, and NEC wrote the manuscript. TGF, PRB, TB, and NEC analyzed the data. JJB scanned fossil material and wrote the associated methods. RDCB created the 3D PDFs. BPK collected fossil material. SW provided access to segmenting software. All authors edited and commented on the manuscript, figures, and tables.

FUNDING

Synchrotron scanning was facilitated by an IMBL beamtime application (15769) awarded to RDCB and TB. RDCB and TB are financed by UNE Postdoctoral Research Fellowships. This study was funded by a UNE Research Training Program Scholarship to TGF and an Australian Research Council Discovery Early Career Award (DE190101423) to NEC.

ACKNOWLEDGMENTS

We thank Mary-Anne Binnie (SAMA) for providing access to study SAMA P40536. Christopher Goatley [University of New England (UNE)] assisted with Micro-CT scanning the *in situ* maxillary tooth. Anton Maksimenko provided technical assistance with the synchrotron scan data through his IMBL-Stitch software. TNT is made freely available thanks to a subsidy from the Willi Hennig Society. Special thanks to members of the Palaeoscience Research Centre at UNE for discussions related to this study, in particular Kai Allison, Marissa Betts, and John Paterson. Finally, we thank W Zheng, RT Tucker, and one anonymous reviewer for their constructive feedback. BPK acknowledges an Australian Research Council Linkage Project grant (LP0453550), which funded the excavation of SAMA P40536.

SUPPLEMENTARY MATERIAL

The Supplementary Material for this article can be found online at: https://www.frontiersin.org/articles/10.3389/feart.2022.803505/full#supplementary-material

REFERENCES

Apesteguía, S., and Gallina, P. A. (2011). Tunasniyoj, a Dinosaur Tracksite from the Jurassic-Cretaceous Boundary of Bolivia. *Acad. Bras. Ciênc.* 83, 267–277. doi:10.1590/S0001-37652011000100015

Arbour, V. M., Burns, M. E., Sullivan, R. M., Lucas, S. G., Cantrell, A. K., Fry, J., et al. (2014a). A New Ankylosaurid Dinosaur from the Upper Cretaceous (Kirtlandian) of New Mexico with Implications for Ankylosaurid Diversity in the Upper Cretaceous of Western North America. *PLoS One* 9, e108804. doi:10.1371/journal.pone.0108804

Arbour, V. M., and Currie, P. J. (2013). *Euoplocephalus tutus* and the Diversity of Ankylosaurid Dinosaurs in the Late Cretaceous of Alberta, Canada, and Montana, USA. *PLoS One* 8 (5), e62421. doi:10.1371/journal.pone.0062421

Arbour, V. M., and Currie, P. J. (2016). Systematics, Phylogeny and Palaeobiogeography of the Ankylosaurid Dinosaurs. *J. Syst. Palaeontology* 14 (5), 385–444. doi:10.1080/14772019.2015.1059985

Arbour, V. M., Currie, P. J., and Badamgarav, D. (2014b). The Ankylosaurid Dinosaurs of the Upper Cretaceous Baruungoyot and Nemegt Formations of Mongolia. *Zoolog. J. Linn. Soc.* 172 (3), 631–652. doi:10.1111/zoj12185

Arbour, V. M., and Evans, D. C. (2017). A New Ankylosaurine Dinosaur from the Judith River Formation of Montana, USA, Based on an Exceptional Skeleton with Soft Tissue Preservation. *R. Soc. Open Sci.* 4 (5), 161086. doi:10.1098/rsos.161086

Arbour, V. M., Zanno, L. E., and Gates, T. (2016). Ankylosaurian Dinosaur Palaeoenvironmental Associations Were Influenced by Extirpation, Sea-Level Fluctuation, and Geodispersal. *Palaeogeogr. Palaeoclimatol. Palaeoecol.* 449, 289–299. doi:10.1016/j.palaeo.2016.02.033

Barrett, P. M., Rich, T. H., Vickers-Rich, P., Tumanova, T. y. A., Inglis, M., Pickering, D., et al. (2010). Ankylosaurian Dinosaur Remains from the Lower Cretaceous of Southeastern Australia. *Alcheringa: Australas. J. Palaeontology* 34 (3), 205–217. doi:10.1080/03115511003655430

Bartholomai, A. L. (2004). The Large Aspidorhynchid Fish, *Richmondichthys sweeti* (Etheridge Jnr and Smith Woodward, 1891) from Albian Marine Deposits of Queensland, Australia. *Mem. Queensl. Mus.* 49 (2), 521–536.

Bartholomai, A. L. (2012). The Pachyrhizodontid Teleosts from the marine Lower Cretaceous (Latest Mid to Late-Albian) Sediments of the Eromanga Basin, Queensland, Australia. *Mem. Queensl. Mus.* 56 (1), 119–147.

Bartholomai, A. L. (2015a). Additional Chimaeroid Specimens from the Early Cretaceous (Late Albian) Toolebuc Formation, Queensland, Australia. *Mem. Queensl. Mus.* 59, 117–185. doi:10.17082/j.2204-1478.59.2015.2015-03

Bartholomai, A. L. (2015b). An Early Cretaceous (Late Albian) Halecomorph (? Ionoscopiformes) Fish from the Toolebuc Formation of the Eromanga Basin. *Mem. Queensl. Mus.* 59, 61–74. doi:10.17082/j.2204-1478.59.2015.2014-05

Bell, P. R., Burns, M. E., and Smith, E. T. (2018a). A Probable Ankylosaurian (Dinosauria, Thyreophora) from the Early Cretaceous of New South Wales, Australia. *Alcheringa: Australas. J. Palaeontology* 42 (1), 120–124. doi:10.1080/03115518.2017.1384851

Bell, P. R., Fanti, F., Hart, L. J., Milan, L. A., Craven, S. J., Brougham, T., et al. (2019). Revised Geology, Age, and Vertebrate Diversity of the Dinosaur-bearing Griman Creek Formation (Cenomanian), Lightning Ridge, New South Wales, Australia. *Palaeogeogr. Palaeoclimatol. Palaeoecol.* 514, 655–671. doi:10.1016/j.palaeo.2018.11.020

Bell, P. R., Herne, M. C., Brougham, T., and Smith, E. T. (2018b). Ornithopod Diversity in the Griman Creek Formation (Cenomanian), New South Wales, Australia. *PeerJ* 6, e6008. doi:10.7717/peerj.6008

Bourke, J. M., Porter, W. R., and Witmer, L. M. (2018). Convoluted Nasal Passages Function as Efficient Heat Exchangers in Ankylosaurs (Dinosauria: Ornithischia: Thyreophora). *PLoS One* 13 (12), e0207381. doi:10.1371/journal.pone.0207381

Brett-Surman, M. K. (1979). Phylogeny and Palaeobiogeography of Hadrosaurian Dinosaurs. *Nature* 277 (5697), 560–562. doi:10.1038/277560a0

Brown, B., and Kaisen, P. C. (1908). The Ankylosauridae, a New Family of Armored Dinosaurs from the Upper Cretaceous. *Bull. AMNH* 24 (12), 187–201.

Burns, M. E., Currie, P. J., Sissons, R. L., and Arbour, V. M. (2011). Juvenile Specimens of *Pinacosaurus grangeri* Gilmore, 1933 (Ornithischia: Ankylosauria) from the Late Cretaceous of China, with Comments on the Specific Taxonomy of *Pinacosaurus*. *Cretaceous Res.* 32 (2), 174–186. doi:10.1016/j.cretres.2010.11.007

Carpenter, K. (2001). "Phylogenetic Analysis of the Ankylosauria," in *The Armored Dinosaurs*. Editor K. Carpenter (Bloomington: Indiana University Press), 455–483.

Carpenter, K. (2004). Redescription of *Ankylosaurus magniventris* Brown 1908 (Ankylosauridae) from the Upper Cretaceous of the Western Interior of North America. *Can. J. Earth Sci.* 41 (8), 961–986. doi:10.1139/E04-043

Carpenter, K., Bartlett, J., Bird, J., and Barrick, R. (2008). Ankylosaurs from the Price River Quarries, Cedar Mountain Formation (Lower Cretaceous), East-central Utah. *J. Vertebr. Paleontol.* 28 (4), 1089–1101. doi:10.1671/0272-4634-28.4.1089

Carpenter, K., Hayashi, S., Kobayashi, Y., Maryańska, T., Barsbold, R., Sato, K., et al. (2011). *Saichania chulsanensis* (Ornithischia, Ankylosauridae) from the Upper Cretaceous of Mongolia. *Palaeontogr. Abt. A* 294 (1-3), 1–61. doi:10.1127/pala/294/2011/1

Carpenter, K., Kirkland, J. I., Burge, D., and Bird, J. (2001a). "Disarticulated Skull of a New Primitive Ankylosaurid from the Lower Cretaceous of Eastern Utah," in *The Amored Dinosaurs*. Editor K. Carpenter (Bloomington: Indiana University Press), 211–238.

Carpenter, K., Miles, C. A., and Cloward, K. (2001b). "New Primitive Stegosaur from the Morrison Formation, Wyoming," in *The Armored Dinosaurs*. Editor K. Carpenter (Bloomington: Indiana University Press), 55–75.

Cavin, L., and Berrell, R. W. (2019). Revision of *Dugaldia emmilta* (Teleostei, Ichthyodectiformes) from the Toolebuc Formation, Albian of Australia, with Comments on the Jaw Mechanics. *J. Vertebr. Paleontol.* 39 (1), e1576049. doi:10.1080/02724634.2019.1576049

Chengkai, J., Foster, C. A., Xing, X., and Clark, J. M. (2007). The First Stegosaur (Dinosauria, Ornithischia) from the Upper Jurassic Shishugou Formation of Xinjiang, China. *Acta Geol. Sin- English Edition* 81 (3), 351–356. doi:10.1111/j.1755-6724.2007.tb00959.x

Chiappe, L. M. (1996). Early Avian Evolution in the Southern Hemisphere: the Fossil Record of Birds in the Mesozoic of Gondwana. *Mem. Queensl. Mus.* 39, 533–556.

Cooling, J. J., Crowley, J. L., McKellar, J. L., Esterle, J. S., Nicoll, R. S., and Bianchi, V. (2021). Stratigraphic Constraints on the Lower Cretaceous Orallo Formation, southeastern Queensland: U-Pb Dating of Bentonite and Palynostratigraphy of Associated Strata. *Aust. J. Earth Sci.* 68 (3), 343–354. doi:10.1080/08120099.2020.1781690

Coria, R. A., and Salgado, L. (2001). "South American Ankylosaurs," in *The Armored Dinosaurs*. Editor K. Carpenter (Bloomington: Indiana University Press), 159–168.

Eaton, T. H., Jr (1960). A New Armored Dinosaur from the Cretaceous of Kansas. *Univ. Kans. Paleontol. Contrib., Vert.* 8, 1–24.

Fletcher, T. L., and Salisbury, S. W. (2010). New Pterosaur Fossils from the Early Cretaceous (Albian) of Queensland, Australia. *J. Vertebr. Paleontol.* 30 (6), 1747–1759. doi:10.1080/02724634.2010.521929

Francischini, H., Sales, M. A. F., Dentzien–Dias, P., and Schultz, C. L. (2018). The Presence of Ankylosaur Tracks in the Guará Formation (Brazil) and Remarks on the Spatial and Temporal Distribution of Late Jurassic Dinosaurs. *Ichnos* 25 (2-3), 177–191. doi:10.1080/10420940.2017.1337573

Gibbons, A. D., Whittaker, J. M., and Müller, R. D. (2013). The Breakup of East Gondwana: Assimilating Constraints from Cretaceous Ocean Basins Around India into a Best-Fit Tectonic Model. *J. Geophys. Res. Solid Earth* 118, 808–822. doi:10.1002/jgrb.50079

Godefroit, P., Pereda-Suberbiola, X., Li, H., and Dong, Z.-M. (1999). A New Species of the Ankylosaurid Dinosaur *Pinacosaurus* from the Late Cretaceous of Inner Mongolia (PR China). *Bulletin de l'Institut Royal des Sciences Naturelles de Belgique, Sciences de la terre*, 69, 17–36.

Goloboff, P. A., and Catalano, S. A. (2016). TNT Version 1.5, Including a Full Implementation of Phylogenetic Morphometrics. *Cladistics* 32 (3), 221–238. doi:10.1111/cla.12160

Gureyev, T. E., Nesterests, Y., Ternovski, D., Thompson, D., Wilkins, S. W., Stevenson, A. W., et al. (2011). Toolbox for Advanced X-ray Image Processing. *Adv. Comput. Methods X-Ray Opt. ll* 8141 (81410B). doi:10.1117/12.893252

Henderson, R. A. (2004). A Mid-Cretaceous Association of Shell Beds and Organic-Rich Shale: Bivalve Exploitation of a Nutrient-Rich, Anoxic Sea-Floor Environment. *Palaios* 19 (2), 156–169. doi:10.1669/0883-1351(2004)019<0156:amaosb>2.0.co;2

Henderson, R. A., Crampton, J. S., Dettman, M. E., Douglas, J. G., Haig, D., Shafik, S., et al. (2000). Biogeographical Observations on the Cretaceous Biota of Australasia. *Mem. Assoc. Australas. Palaeontologists* 23, 355–404.

Hill, R. V., Witmer, L. M., and Norell, M. A. (2003). A New Specimen of *Pinacosaurus grangeri* (Dinosauria: Ornithischia) from the Late Cretaceous of Mongolia: Ontogeny and Phylogeny of Ankylosaurs. *Am. Mus. Novitates* 3395, 1–29. doi:10.1206/0003-0082(2003)395<0001:ansopg>2.0.co;2

Ibiricu, L. M., Casal, G. A., Alvarez, B. N., De Sosa Tomas, A., Lamanna, M. C., and Cruzado-Caballero, P. (2021). New Hadrosaurid (Dinosauria: Ornithopoda) Fossils from the Uppermost Cretaceous of central Patagonia and the Influence of Paleoenvironment on South American Hadrosaur Distribution. *J. South Am. Earth Sci.* 110, 103369. doi:10.1016/j.jsames.2021.103369

Jiang, K., Lin, C., Zhang, X., He, W., and Xiao, F. (2018). Geochemical Characteristics and Possible Origin of Shale Gas in the Toolebuc Formation in the Northeastern Part of the Eromanga Basin, Australia. *J. Nat. Gas Sci. Eng.* 57, 68–76. doi:10.1016/j.jngse.2018.06.031

Kear, B. P. (2003). Cretaceous marine Reptiles of Australia: a Review of Taxonomy and Distribution. *Cretaceous Res.* 24 (3), 277–303. doi:10.1016/S0195-6671(03)00046-6

Kear, B. P. (2006). First Gut Contents in a Cretaceous Sea Turtle. *Biol. Lett.* 2, 113–115. doi:10.1098/rsbl.2005.0374

Kear, B. P. (2007). First Record of a Pachycormid Fish (Actinopterygii: Pachycormiformes) from the Lower Cretaceous of Australia. *J. Vertebr. Paleontol.* 27 (4), 1033–1038. doi:10.1671/0272-4634(2007)27[1033:froapf]2.0.co;2

Kear, B. P. (2016). Cretaceous marine Amniotes of Australia: Perspectives on a Decade of New Research. *Mem. Vic. Mus* 74, 17–28. doi:10.24199/j.mmv.2016.74.03

Kear, B. P., Boles, W. E., and Smith, E. T. (2003). Unusual Gut Contents in a Cretaceous Ichthyosaur. *Proc. R. Soc. Lond. B* 270, S206–S208. doi:10.1098/rsbl.2003.0050

Kear, B. P., Fordyce, R. E., Hiller, N., and Siversson, M. (2018). A Palaeobiogeographical Synthesis of Australasian Mesozoic Marine Tetrapods. *Alcheringa: Australas. J. Palaeontology* 42 (4), 461–486. doi:10.1080/03115518.2017.1397428

Kear, B. P., and Hamilton-Bruce, R. J. (2011). "Dinosaurs in Australia," in *Mesozoic Life from the Southern Continent* (Melbourne: CSIRO Publishing), 190. doi:10.1071/9780643101692

Kear, B. P., and Lee, M. S. Y. (2006). A Primitive Protostegid from Australia and Early Sea Turtle Evolution. *Biol. Lett.* 2 (1), 116–119. doi:10.1098/rsbl.2005.0406

Kellner, A. W. A., Rich, T. H., Costa, F. R., Vickers-Rich, P., Kear, B. P., Walters, M., et al. (2010). New Isolated Pterodactyloid Bones from the Albian Toolebuc Formation (Western Queensland, Australia) with Comments on the Australian Pterosaur Fauna. *Alcheringa: Australas. J. Palaeontology* 34 (3), 219–230. doi:10.1080/03115511003656552

Kellner, A. W. A., Rodrigues, T., and Costa, F. R. (2011). Short Note on a Pteranodontoid Pterosaur (Pterodactyloidea) from Western Queensland, Australia. *Acad. Bras. Ciênc.* 83 (1), 301–308. doi:10.1590/s0001-37652011000100018

Kemp, A. (1993). Ceratodus Diutinus, a New Ceratodont from Cretaceous and Late Oligocene-Medial Miocene Deposits in Australia. *J. Paleontol.* 67 (5), 883–888. doi:10.1017/s0022336000037148

Kilbourne, B., and Carpenter, K. (2005). Redescription of *Gargoyleosaurus parkpinorum*, a Polacanthid Ankylosaur from the Upper Jurassic of Albany County, Wyoming. *Neues Jahrb. Geol. PalĘontol., Abh.* 235 (1), 111–160. doi:10.1127/njgpa/235/2005/111

Kinneer, B., Carpenter, K., and Shaw, A. (2016). Redescription of *Gastonia Burgei* (Dinosauria: Ankylosauria, Polacanthidae), and Description of a New Species. *Neues Jahrb. Geol. PalĘontol., Abh.* 282 (1), 37–80. doi:10.1127/njgpa/2016/0605

Kirkland, J. I. (1998). A Polacanthine Ankylosaur (Ornithischia: Dinosauria) from the Early Cretaceous (Barremian) of Eastern Utah. *New Mexico Mus. Nat. Hist. Sci. Bull.* 14, 271–281.

Kubo, T. (2020). Biogeographical Network Analysis of Cretaceous Australian Dinosaurs. *Gondwana Res.* 82, 39–47. doi:10.1016/j.gr.2019.12.012

Kurochkin, E. N., and Molnar, R. E. (1997). New Material of Enantiornithine Birds from the Early Cretaceous of Australia. *Alcheringa: Australas. J. Palaeontology* 21 (4), 291–297. doi:10.1080/03115519708619169

Leahey, L. G., Molnar, R. E., Carpenter, K., Witmer, L. M., and Salisbury, S. W. (2015). Cranial Osteology of the Ankylosaurian Dinosaur Formerly Known as *Minmi* sp. (Ornithischia: Thyreophora) from the Lower Cretaceous Allaru Mudstone of Richmond, Queensland, Australia. *PeerJ* 3, e1475. doi:10.7717/peerj.1475

Leahey, L. G., and Salisbury, S. W. (2013). First Evidence of Ankylosaurian Dinosaurs (Ornithischia: Thyreophora) from the Mid-Cretaceous (Late Albian-Cenomanian) Winton Formation of Queensland, Australia. *Alcheringa: Australas. J. Palaeontology* 37 (2), 249–257. doi:10.1080/03115518.2013.743703

Lee, Y.-N. (1996). A New Nodosaurid Ankylosaur (Dinosauria: Ornithischia) from the Paw Paw Formation (Late Albian) of Texas. *J. Vertebr. Paleontol.* 16 (2), 232–245. doi:10.1080/02724634.1996.10011311

Lees, T. A. (1986). A New Chimaeroid *Ptyktoptychion tayyogen*. et sp. nov. (Pisces: Holocephali) from the Marine Cretaceous of Queensland. *Alcheringa: Australas. J. Palaeontology* 10 (3), 187–193. doi:10.1080/03115518608619154

Lü, J., Jin, X., Sheng, Y., Li, Y., Wang, G., and Azuma, Y. (2007). New Nodosaurid Dinosaur from the Late Cretaceous of Lishui, Zhejiang Province, China. *Acta Geologica Sinica* 83, 344–350.

Maddison, W. P., and Maddison, D. R. (2019). Mesquite: a Modular System for Evolutionary Analysis. Available at: http://www.mesquiteproject.org.

Maidment, S. C. R., Strachan, S. J., Ouarhache, D., Scheyer, T. M., Brown, E. E., Fernandez, V., et al. (2021). Bizarre Dermal Armour Suggests the First African Ankylosaur. *Nat. Ecol. Evol.* 5, 1576–1581. doi:10.1038/s41559-021-01553-6

Maidment, S. C. R., Woodruff, D. C., and Horner, J. R. (2018). A New Specimen of the Ornithischian Dinosaur *Hesperosaurus mjosi* from the Upper Jurassic Morrison Formation of Montana, U.S.A., and Implications for Growth and Size in Morrison Stegosaurs. *J. Vertebr. Paleontol.* 38 (1), e1406366. doi:10.1080/02724634.2017.1406366

Mateus, O., Maidment, S. C. R., and Christiansen, N. A. (2009). A New Long-Necked "sauropod-Mimic" Stegosaur and the Evolution of the Plated Dinosaurs. *Proc. R. Soc. B.* 276 (1663), 1815–1821. doi:10.1098/rspb.2008.1909

McMinn, A., and Burger, D. (1986). Palynology and Palaeoenvironment of the Toolebuc Formation (Sensu Lato) in the Eromanga Basin. Contributions to the Geology and Hydrocarbon Potential of the Eromanga Basin. Editors D. I. Gravestock, P. S. Moore, and G. M. Pitt (Sydney: Geological Society of Australia), 139–154.

Molnar, R. E. (1980). An Ankylosaur (Ornithschia: Reptilia) from the Lower Cretaceous of Southern Queensland. *Mem. Queensl. Mus.* 20, 77–87.

Molnar, R. E. (1986). An Enantiornithine Bird from the Lower Cretaceous of Queensland, Australia. *Nature* 322, 736–738. doi:10.1038/322736a0

Molnar, R. E. (1987). A Pterosaur Pelvis from Western Queensland, Australia. *Alcheringa: Australas. J. Palaeontology* 11 (2), 87–94. doi:10.1080/03115518708618981

Molnar, R. E. (1996). Preliminary Report a New Ankylosaur from the Early Cretaceous of Queensland, Australia. *Mem. Queensl. Mus.* 39 (3), 653–668.

Molnar, R. E. (2001). Armor of the Small Ankylosaur *Minmi*, in *The Armored Dinosaurs*. Editor K. Carpenter (Bloomington: Indiana University Press), 341–363.

Molnar, R. E., and Thulborn, R. A. (1980). First Pterosaur from Australia. *Nature* 288, 361–363. doi:10.1038/288361a0

Molnar, R. E., and Wiffen, J. (1994). A Late Cretaceous Polar Dinosaur Fauna from New Zealand. *Cretaceous Res.* 15 (6), 689–706. doi:10.1006/cres.1994.1038

Moore, P. S., Pitt, G. M., and Dettman, M. E. (1986). The Early Cretaceous Coorikiana Sandstone and Toolebuc Formation: Their Recognition and Stratigraphic Relationship in the Southwestern Eromanga Basin, in *Contributions to the Geology and Hydrocarbon Potential of the Eromanga Basin*. Editors D. I. Gravestock, P. S. Moore, and G. M. Pitt (Sydney: Geological Society of Australia), 97–114.

Murray, A., Riguetti, F., and Rozadilla, S. (2019). New Ankylosaur (Thyreophora, Ornithischia) Remains from the Upper Cretaceous of Patagonia. *J. South Am. Earth Sci.* 96, 102320. doi:10.1016/j.jsames.2019.102320

Nopcsa, F. (1915). Die Dinosaurier der siebenbürgischen Landesteile Ungarns. *Mitteilungen aus dem Jahrbuche der Königlich-Ungarischen Geologischen Reichsanstalt* 23, 1–26.

Norman, D. B. (2020). *Scelidosaurus harrisonii* from the Early Jurassic of Dorset, England: Cranial Anatomy. *Zoolog. J. Linn. Soc.* 188 (1), 1–81. doi:10.1093/zoolinnean/zlz074

Osborn, H. F. (1923). Two Lower Cretaceous Dinosaurs from Mongolia. *Am. Mus. Novitates* 95, 1–10.

Ősi, A. (2005). *Hungarosaurus tormai*, a New Ankylosaur (Dinosauria) from the Upper Cretaceous of Hungary. *J. Vertebr. Paleontol.* 25 (2), 370–383. doi:10.1671/0272-4634(2005)025[0370:HTANAD]2.0.CO;2

Owen, R. (1842). Report on British Fossil Reptiles Part ll. *Report of the British Association for the Advancement of Science* 1841, 60–204.

Park, J.-Y., Lee, Y.-N., Currie, P. J., Kobayashi, Y., Koppelhus, E., Barsbold, R., et al. (2020). Additional Skulls of *Talarurus plicatospineus* (Dinosauria: Ankylosauridae) and Implications for Paleobiogeography and Paleoecology of Armored Dinosaurs. *Cretaceous Res.* 108, 104340. doi:10.1016/j.cretres.2019.104340

Parsons, W. L., and Parsons, K. M. (2009). A New Ankylosaur (Dinosauria: Ankylosauria) from the Lower Cretaceous Cloverly Formation of central Montana. *Can. J. Earth Sci.* 46 (10), 721–738. doi:10.1139/E09-045

Paulina-Carabajal, A., Lee, Y.-N., and Jacobs, L. L. (2016). Endocranial Morphology of the Primitive Nodosaurid Dinosaur *Pawpawsaurus campbelli* from the Early Cretaceous of North America. *PLoS One* 11 (3), e0150845. doi:10.1371/journal.pone.0150845

Paulina-Carabajal, A., Lee, Y.-N., Kobayashi, Y., Lee, H.-J., and Currie, P. J. (2018). Neuroanatomy of the Ankylosaurid Dinosaurs *Tarchia teresae* and *Talarurus plicatospineus* from the Upper Cretaceous of Mongolia, with Comments on Endocranial Variability Among Ankylosaurs. *Palaeogeogr. Palaeoclimatol. Palaeoecol.* 494, 135–146. doi:10.1016/j.palaeo.2017.11.030

Pentland, A. H., and Poropat, S. F. (2019). Reappraisal of *Mythunga Camara* Molnar & Thulborn, 2007 (Pterosauria, Pterodactyloidea, Anhangueria) from the Upper Albian Toolebuc Formation of Queensland, Australia. *Cretaceous Res.* 93, 151–169. doi:10.1016/j.cretres.2018.09.011

Pol, D., and Escapa, I. H. (2009). Unstable Taxa in Cladistic Analysis: Identification and the Assessment of Relevant Characters. *Cladistics* 25 (5), 515–527. doi:10.1111/j.1096-0031.2009.00258.x

Porro, L. B., Witmer, L. M., and Barrett, P. M. (2015). Digital Preparation and Osteology of the Skull of *Lesothosaurus diagnosticus* (Ornithischia: Dinosauria). *PeerJ* 3, e1494. doi:10.7717/peerj.1494

Prieto-márquez, A. (2010). Global Historical Biogeography of Hadrosaurid Dinosaurs. *Zoolog. J. Linn. Soc.* 159 (2), 503–525. doi:10.1111/j.1096-3642.2010.00642.x

Riguetti, F., Citton, P., Apesteguía, S., Zacarías, G. G., and Pereda-Suberbiola, X. (2021). New Ankylosaurian Trackways (Cf. *Tetrapodosaurus*) from an Uppermost Cretaceous Level of the El Molino Formation of Bolivia. *Cretaceous Res.* 124, 104810. doi:10.1016/j.cretres.2021.104810

Rozefelds, A. C. (1993). Lower Cretaceous Anacoracidae? (Lamniformes: Neoselachii); Vertebrae and Associated Dermal Scales from Australia. *Alcheringa: Australas. J. Palaeontology* 17 (3), 199–210. doi:10.1080/03115519308619604

Russel, D., Russel, D., Taquet, P., and Thomas, H. (1976). New Collections of Vertebrates in the Upper Cretaceous Continental Terrains of the Majunga Region (Madagascar). *Comptes Rendus de la Société Geologique de France* 5, 205–208.

Salgado, L., and Gasparini, Z. (2006). Reappraisal of an Ankylosaurian Dinosaur from the Upper Cretaceous of James Ross Island (Antarctica). *Geodiversitas* 28 (1), 119–135.

Salisbury, S. W., Romilio, A., Herne, M. C., Tucker, R. T., and Nair, J. P. (2016). The Dinosaurian Ichnofauna of the Lower Cretaceous (Valanginian-Barremian) Broome Sandstone of the Walmadany Area (James Price Point), Dampier Peninsula, Western Australia. *J. Vertebr. Paleontol.* 36 (Suppl. 1), 1–152. doi:10.1080/02724634.2016.1269539

Seeley, H. G. (1888). Classification of the Dinosauria. *Geol. Mag.* 5 (1), 45–46. doi:10.1017/s0016756800156006

Sereno, P. C. (1999). The Evolution of Dinosaurs. *Science* 284 (5423), 2137–2147. doi:10.1126/science.284.5423.2137

Sereno, P. C., and Zhimin, D. (1992). The Skull of the Basal Stegosaur *Huayangosaurus taibaii* and a Cladistic Diagnosis of Stegosauria. *J. Vertebr. Paleontol.* 12 (3), 318–343. doi:10.1080/02724634.1992.10011463

Soto-Acuña, S., Vargas, A. O., Kaluza, J., Leppe, M. A., Palma-Liberona, J., et al. (2021). Bizarre Tail Weaponry in a Transitional Ankylosaur from Subantarctic Chile. *Nature* 600, 259–263. doi:10.1038/s41586-021-04147-1

Thompson, R. S., Parish, J. C., Maidment, S. C. R., and Barrett, P. M. (2012). Phylogeny of the Ankylosaurian Dinosaurs (Ornithischia: Thyreophora). *J. Syst. Palaeontology* 10 (2), 301–312. doi:10.1080/14772019.2011.569091

Vickaryous, M. K. (2006). New Information on the Cranial Anatomy of *Edmontonia rugosidens* Gilmore, a Late Cretaceous Nodosaurid Dinosaur from Dinosaur Provincial Park, Alberta. *J. Vertebr. Paleontol.* 26 (4), 1011–1013. doi:10.1671/0272-4634(2006)26[1011:niotca]2.0.co;2

Vickaryous, M. K., Maryanska, T., and Weishampel, D. B. (2004). "Ankylosauria," in *The Dinosauria*. second edition Editors D. B. Weishampel, P. Dodson, and H. Osmólska (Berkeley: University of California Press), 363–392. doi:10.1525/california/9780520242098.003.0020

Vickaryous, M. K., Russell, A. P., Currie, P. J., and Zhao, X.-J. (2001). A New Ankylosaurid (Dinosauria: Ankylosauria) from the Lower Cretaceous of China, with Comments on Ankylosaurian Relationships. *Can. J. Earth Sci.* 38 (12), 1767–1780. doi:10.1139/e01-051

Wagstaff, B. E., Gallagher, S. J., Hall, W. M., Korasidis, V. A., Seegets-Villiers, D. E., Vickers-Rich, P. A., et al. (2020). Palynological-age Determination of Early Cretaceous Vertebrate-Bearing Beds along the South Victorian Coast of Australia, with Implications for the Spore-Pollen Biostratigraphy of the Region. *Alcheringa: Australas. J. Palaeontology* 44 (3), 460–474. doi:10.1080/03115518.2020.1754464

Wiersma, J. P., and Irmis, R. B. (2018). A New Southern Laramidian Ankylosaurid, *Akainacephalus johnsoni* gen. et sp. nov., from the Upper Campanian Kaiparowits Formation of Southern Utah, USA. *PeerJ* 6, e5016. doi:10.7717/peerj.5016

Wilson, G. D. F., Paterson, J. R., and Kear, B. P. (2011). Fossil Isopods Associated with a Fish Skeleton from the Lower Cretaceous of Queensland, Australia - Direct Evidence of a Scavenging Lifestyle in Mesozoic Cymothoida. *Palaeontology* 54, 1053–1068. doi:10.1111/j.1475-4983.2011.01095.x

Witmer, L. M., and Ridgely, R. C. (2008). The Paranasal Air Sinuses of Predatory and Armored Dinosaurs (Archosauria: Theropoda and Ankylosauria) and Their Contribution to Cephalic Structure. *Anat. Rec.* 291 (11), 1362–1388. doi:10.1002/ar.20794

Yang, J., You, H., Xie, L., and Zhou, H. (2017). A New Specimen of *Crichtonpelta benxiensis* (Dinosauria: Ankylosaurinae) from the Mid-cretaceous of Liaoning Province, China. *Acta Geol. Sin.* 91 (3), 781–790. doi:10.1111/1755-6724.13308

Zammit, M., Norris, R. M., and Kear, B. P. (2010). The Australian Cretaceous Ichthyosaur *Platypterygius australis*: a Description and Review of Postcranial Remains. *J. Vertebr. Paleontol.* 30 (6), 1726–1735. doi:10.1080/02724634.2010.521930

Conflict of Interest: The authors declare that the research was conducted in the absence of any commercial or financial relationships that could be construed as a potential conflict of interest.